

Annu. Rev. Astron. Astrophys. 1991. 29: 627–84
Copyright © 1991 by Annual Reviews Inc. All rights reserved

SEISMIC OBSERVATIONS OF THE SOLAR INTERIOR

Douglas Gough

Institute of Astronomy and Department of Applied Mathematics and
Theoretical Physics, University of Cambridge, Cambridge CB3 0HA,
England

Juri Toomre

Joint Institute for Laboratory Astrophysics and Department of
Astrophysical, Planetary and Atmospheric Sciences,
University of Colorado, Boulder, CO 80309

KEY WORDS: helioseismology, solar structure, solar rotation

1. INTRODUCTION

The sun is oscillating in an intricate manner. The patterns of motion observed in the solar atmosphere result in part from interference between about 10^7 resonant modes of oscillation of the interior. The rich spectrum of the detected oscillations arises from modes with periods ranging from a few minutes to several hours and with horizontal wavelengths of between less than a few thousand kilometers to global scales. Each mode can be regarded as a resonant standing wave whose traveling constituents propagate in a well defined spherical shell in the solar interior. The lower boundary of the shell, depending on the mode, could be quite shallow or could be essentially at the center of the star. For many modes the upper boundary is not far beneath the photosphere. These modes can tunnel through the overlying evanescent region into the visible atmosphere where they can be detected. Since the frequencies of the modes are determined principally by the stratification and dynamics of that portion of the sun where the amplitudes are appreciable, accurate frequency measurements provide data that enable us to probe the sun's interior structure. During

the past decade there has been significant progress in both observation and theory. Here, we assess what has been learned and what puzzles have emerged. The unravelling of information from many modes forms the basis of a new subject: helioseismology.

An essential difference between helioseismology and the study of the classical pulsating stars is in the number and amplitude of detectable modes. Detailed inferences about the internal structure, composition, and motions can be drawn for the sun, whereas when only a single or at most a few modes are available such inferences are not feasible. However, it is likely that at least solar-type stars pulsate in a manner similar to the sun, and that the detection and measurement of the frequencies of a substantial number of the largest-scale modes will soon be possible. Therefore one can anticipate imminent progress in asteroseismology, though the resolution of the structures of other stars will necessarily be less precise. An important property of solar-type oscillations is that their amplitudes are small; linear theory can therefore be used, and because the salient aspects of that theory are quite well understood, one can reasonably expect that powerful new constraints will soon be imposed on the possible properties of stars.

It is hoped that many of the techniques developed in helioseismology can be carried over to studies of a wide range of main-sequence stars, and even to stars late in their evolution, such as red giants and white dwarfs. Of course, the faintness of the sources introduces new challenges. Advances in asteroseismology will hinge on obtaining large telescopes dedicated for long intervals to seismic observations, along with new breeds of stable and sensitive detectors. Although these may not be readily available, the scientific rewards are likely to be great. Judging by what has already been learned about the sun, and what seems to be in the offing in the near future, we surmise that asteroseismology will provide ways of probing the interiors of stars that can be achieved by no other means.

Our purpose here is to assess what has been accomplished in helioseismology during the past seven years since the previous report in *Annual Reviews* (95). We shall not review the beginnings of this subject in any detail, nor dwell on basic explanations of the physics of the oscillations. Comprehensive reviews covering those subjects are already available (39, 43, 54, 56, 70, 95, 150, 155, 177, 228, 232, 314, 315, 327), as are proceedings of seven recent conferences listed in the literature citations.

We should, however, at least recall that the study of solar oscillations began in 1960 with the discovery (230, 231) that about half of the solar surface is occupied by patches that appear to oscillate intermittently with periods near 5 minutes and with amplitudes of about 1 km s^{-1} . These “5-minute oscillations” were at first regarded as local disturbances, possibly initiated by turbulent convection erupting into the atmosphere. In 1970,

following a suggestion by Frazier (127a), the real explanation was offered by Ulrich (317) and independently by Leibacher & Stein (229), who proposed that the oscillations are the superposition of resonant acoustic modes of the interior. In 1975 the dependence of the eigenfrequencies on horizontal wavelengths predicted by linearized theory (1, 317) was confirmed by the observations of Deubner (94). Within a year other observations (35, 195, 290), using a variety of techniques, suggested that oscillations with much longer periods (20–60 min, 160 min) were also present. Helioseismology then began in earnest, aided particularly by the remarkable power spectra obtained from whole-disk Doppler observations (75, 171).

The first helioseismic inferences were drawn from a direct comparison of observed frequencies with theoretical predictions, and from interpreting the differences in the light of simple models and analytical asymptotic formulae. Thus it was deduced immediately from Deubner's data that the sun's convection zone is some 50% deeper than the convection zones in theoretical models of the time (147), and, from the whole-disk data, that the solar helium abundance is certainly not as low as would have been required to reproduce the observed neutrino flux from standard theoretical models (64). An outcome of the comparison with whole-disk data is that it was not possible to reproduce theoretically the whole range of the observed frequencies. Although early asymptotic arguments permitted one to estimate qualitatively from the discrepancies both where and in what respect the theoretical models were in error, it was not until inverse calculations were performed that reliable quantitative estimates could be made.

The major accomplishments of the last seven years have been in establishing the angular velocity Ω and the spherically symmetrical part of the adiabatic sound speed c throughout much of the interior of the sun. Contrary to many theoretical predictions, we now know that Ω does not increase rapidly with depth in the radiative interior, except possibly in the central energy-generating core. Consequently the quadrupole moment of the sun's exterior gravitational field, together with planetary ranging data, are consistent with General Relativity. We know also that c is some 1% greater than predictions in the mid-regions of the radiative envelope; this suggested that opacities had been underestimated immediately beneath the convection zone, a prediction which has since been confirmed by more careful opacity calculations. In addition we know the depth of the adiabatically stratified region of the convection zone to better than 0.5% of the solar radius.

As we discuss in this review, substantial progress has been made in our quest to ascertain the helium abundance of the material in the convection

zone. Moreover, we have evidence that a recent relatively sophisticated equation of state is a better approximation to reality than older descriptions, and we have some clues about the location of the major structural changes that take place in the sun during the solar cycle. In addition, there has been progress in our understanding of the mechanisms that excite, absorb, and scatter the waves that constitute the acoustic modes; one can anticipate that in the future this understanding will add to our diagnostic capability.

2. SOLAR EVOLUTION

Before embarking on a discussion of seismic diagnosis it is instructive to briefly survey those properties of theoretical models of the sun that might be tested. To get a sense of the reliability of the models, we also record the principal assumptions upon which the theory stands. We postpone discussion of these assumptions until later in the review.

On the Construction of Standard Solar Models

The structure of the sun is estimated from the theory of stellar evolution by integrating a model of a star with a solar mass usually from its zero-age main-sequence state to the present. Many explicit simplifying assumptions render the model uncertain; the most serious of which are:

- uniform initial chemical composition,
- no macroscopic motion aside from convection; zero angular velocity,
- no diffusive mixing of material outside the convection zone,
- no segregation of chemical elements,
- no wave transport of material or energy,
- no mass loss nor accretion,
- no magnetic fields,
- hydrostatic balance,
- thermal balance,
- sun spherically symmetrical throughout its evolution,
- age known,
- Newtonian gravitation: constant G ,
- standard properties of elementary particles.

Added to these are the uncertainties in the microscopic physics from which the equation of state, the opacity, and the nuclear reaction rates are computed.

The uniformity of the initial chemical composition was originally justified by the belief that during its contraction to the main sequence, the sun had passed through a fully convective Hayashi phase. Even after

computations by Larson (225) suggested that the convective envelope might never have penetrated right to the center of the sun, the custom has continued, principally for simplicity. Minor chemical inhomogeneities arising from nuclear reactions that take place during the approach to the main sequence influence the structure of the core at the time, but their influence on the model of the present sun is hardly perceptible (201). Therefore, at least at first we can ignore them. However, substantial inhomogeneities in the initial abundances X_0 , Y_0 and Z_0 of hydrogen, helium, and heavy elements that survive the Hayashi phase have been suggested (199); these could have had a profound effect on the present structure of the sun. Gravitational settling leading to a helium-rich core has also been discussed (79, 92, 245, 323, 328, 329).

Large-scale macroscopic motion is probably ignored simply because we do not know how to compute it (309). The same is true for magnetic fields, mass loss and accretion, and of material and energy transport by small-scale motion. With the burden of such ignorance it was found desirable to have a simple solar model in which such possibilities are excluded, to provide an example against which to compare more complicated models. It was perhaps out of that desire that the concept of a so-called standard solar model arose. This is not a standard in the usual sense, for there are many different such models and their structures are rarely available to the community; the term has been adopted by some workers merely to describe any model computed under assumptions similar to those listed above.

We must emphasize that many of the assumptions are not wholly arbitrary. They have, from time to time, been assessed (e.g. 277). Moreover, even if they are incorrect, their impact on stellar evolution theory generally appears to be subtle, because broadly speaking the theory has been able to successfully describe most of the characteristics of stellar evolution that can be tested by astronomical observations.

Granted for the moment that the solar model is not seriously unstable, and knowing that the characteristic time scale over which thermonuclear reactions modify the chemical composition of the core is much greater than the thermal diffusion time, it is to be expected that the model is in thermal balance. Indeed, most evolution calculations can accommodate a spherically symmetrical thermal imbalance, and naturally find it to be small. However, modern calculations (29, 59, 216a, 280, 297) do find the sun to be unstable to aspherical perturbations, the nonlinear development of which is not understood. Hydrostatic balance is usually assumed explicitly; the sun does not currently pulsate with a substantial amplitude, nor do other solar-type main-sequence stars younger than the sun. Furthermore, spherical symmetry is the most natural assumption to adopt for the simple standard model. It appears that under such conditions the model

is probably uniquely determined once the chemical composition is specified and a means for describing the stratification of the convection zone is provided. The sole purpose of evolving the model in time, therefore, is to follow the nuclear reactions to determine how the abundances of principally hydrogen and helium have been modified from their assumed initial uniform values.

In the light of this conclusion one can readily appreciate the implications of assuming no macroscopic motion other than convection: Since the core is found to be stable to convection, the products of the nuclear reactions are forced to remain in situ. Moreover, the neglect of any material diffusion implies that nuclear reactions provide the only process whereby chemical abundances can be modified.

Finally, a word about convection: It is assumed that convective transport takes place wherever the stratification of the star is found to be locally unstable to convection. That is the only stability criterion that is recognized when constructing the standard models. Convection is taken into account partly because it is observed to occur beneath the photosphere of the sun and partly because of its importance in controlling the radius of the model. Indeed, without convection it would not even be possible to construct a model of the sun with the observed solar radius. Usually a local relation between heat flux and temperature gradient based on a mixing-length formalism is used; for the purposes of modeling the interior of the sun the details of the relation hardly matter, provided the formula for the heat flux is an increasing function of temperature gradient and contains an adjustable parameter α to control the efficacy of the transport of heat (170). Reynolds stresses are usually but not always ignored.

Calibrating the Models

Solar models must be calibrated so that they have the observed radius R_\odot and luminosity L_\odot at the presumed age t_\odot . This is accomplished by adjusting the initial chemical composition and the mixing-length parameter α . Since there are three independent parameters to adjust (namely α and initial relative abundances by mass Y_\odot and Z_\odot , say, of helium and heavy elements), and only two quantities to reproduce, an additional relation must be imposed. Usually either Z_\odot is specified, or the ratio Z_\odot/X_\odot is chosen from astronomical evidence (e.g. 11, 13), where $X_\odot = 1 - Y_\odot - Z_\odot$ is the initial hydrogen abundance. For the purposes of computation, however, it is Z_\odot that must be specified, because opacity tables are written at constant Z_\odot . Bahcall & Ulrich (13), for example, have obtained a desired value of Z_\odot/X_\odot by interpolation between opacity tables computed with different values of Z . Further iteration is hardly necessary because astronomical estimates of Z_\odot/X_\odot are imprecise.

Properties of the Models

An indication of the structure of solar models is given in Figure 1. Depicted is the square of the sound speed c^2 , which is an indication of temperature, plotted against fractional radius r/R , where R is the radius of the model. We show the sound speed because it is the quantity measured by acoustic modes.

As the model evolves on the main sequence, hydrogen is converted into helium in the core. As a consequence, the mean molecular weight increases, and the increase is manifest in Figure 1 as a dip in the sound speed that develops towards the center of the star. Moreover, the core and its immediate environment contract, and the temperature T of the material rises. Contrarily, the envelope expands, increasing R . The expansion more than compensates for the rising temperature, in the sense that at constant r/R the sound speed diminishes. At the center of the model the competing influences of the depletion of fuel and the rising T on the reaction rates largely compensate, so that the central hydrogen abundance X_c decreases almost linearly with time t . In the outer regions of the core there is relatively little hydrogen depletion, so the rising temperature causes the reaction rates to increase. Therefore the integrated energy generation rate L_n rises.

In Figure 1 is also shown a model with low helium and heavy-element abundances. Such models have low neutrino fluxes, nearly consistent with the measurements of Davis and his collaborators (8, 90), and the more

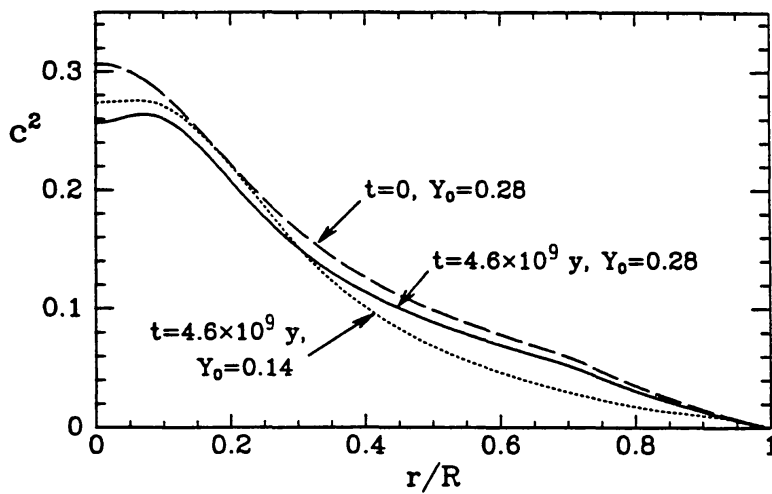


Figure 1 Square of sound speed, c^2 , plotted against relative radius r/R in three solar models. The *continuous line* represents a standard model at the current time ($t = 4.6$ Gy) with $Z = 0.02$, $Y_0 = 0.28$; the *dotted line* represents an initially helium-deficient model ($Z = 0.004$, $Y_0 = 0.14$), also at the current time; the *dashed line* represents the model with $Z = 0.02$, $Y_0 = 0.28$ on the zero-age main sequence. The sound speed c is measured in Mm s^{-1} .

recent measurements from Kamiokande (196). However, as we point out later, these models are ruled out by the seismic data. Decreasing Y increases the abundance X of hydrogen, and therefore requires temperatures to be lower in order to maintain L_n at the observed luminosity L_\odot . In the radiative envelope of the model, where $r > 0.3R$ for instance, increasing Y is somewhat like aging. However, in the convection zone of the helium-deficient model the trend is reversed, and in the core, composition and age variation can be distinguished by the variation in molecular weight.

3. PROPERTIES OF MODES

To a first approximation the sun may be considered to be spherically symmetrical. In that case separable oscillation eigenfunctions with respect to spherical polar coordinates (r, θ, ϕ) can be found. The displacement ξ can be written

$$\xi = \left(\Xi_{nl} P_l^m, \quad \frac{H_{nl}}{L} \frac{dP_l^m}{d\theta}, \quad \frac{H_{nl}}{L \sin \theta} P_l^m \frac{\partial}{\partial \phi} \right) \cos(m\phi - \omega_{nl}t) \quad 3.1$$

where the eigenfunctions Ξ_{nl} , H_{nl} are functions of radius r alone, $P_l^m(\cos \theta)$ is the associated Legendre function of the first kind of degree l and order m , $L^2 = l(l+1)$, and t is time. We refer to the integers l and m as the *degree* and *azimuthal order* of the mode, respectively. The eigenfunctions are also labeled with the integer n , called the *order* of the mode, in such a way that ω_{nl} increases with n at fixed l . The frequencies ω_{nl} also increase with l at fixed n (56, 57); they are degenerate with respect to m . The group of degenerate, or as is actually the case, nearly degenerate (because the sun is not precisely spherical) modes of like n and l is called a *multiplet*, each member of which is a *singlet*.

The classification of the modes is discussed in (95). As Cowling (78) first pointed out, the modes fall into essentially two classes, one of high frequency and the other of low frequency. In the case of polytropes, which Cowling studied, the distinction between the classes is reasonably clear: the low-frequency modes are *internal gravity modes* (g modes) for which buoyancy dominates the restoring force; the high-frequency modes (p modes) are *acoustic modes* for which pressure perturbations provide the main restoring force. If the polytropic index is not too high, these two sequences have increasing numbers of zeros in $\Xi_{nl}(r)$ as $|n|$ increases, and indeed it is possible to choose the origin of n such that $|n|$ is the number of zeros. Then $n > 0$ for p modes and $n < 0$ for g modes. For polytropes of high index, and for realistic models of the sun, this relation between n and the number of zeros does not always hold when l and n are both small,

though it appears to hold otherwise. Discussions of how n is related to the structure of the eigenfunction, based on work of Eckart (114), are given by Scuflaire (286), Osaki (256), and Unno et al (322).

There remain the modes with $n = 0$. These have no nodes for low-index polytropes, or when l is large. In the latter case their nature is clear: They are surface gravity modes which are confined to the outer layers of the sun. Thus Cowling called them *f modes*, for *fundamental (gravity) modes*.

Spherically symmetrical ($l = 0$) modes are a more restricted class. They exhibit no horizontal variation, so gravity modes cannot exist, and only the *p modes* ($n > 0$) are present.

It is common practice to disregard the sign of n , treating it always as a positive number, and to designate the modes as *g*, *f*, or *p*: thus $g_7(l = 2)$ has order -7 and degree 2 according to the foregoing discussion, but is referred to as a *g mode* of order 7; $p_9(l = 3)$ has order 9 and degree 3. We shall adopt this nomenclature in the rest of our discussion. We shall also omit the subscripts n , l from Ξ , H and ω , unless it is ambiguous to do so.

We now summarize briefly some salient properties of the modes of oscillation in terms of asymptotic properties. More detailed discussions are given in (54, 56, 81, 160, 295, 322, 327).

Asymptotic Relations

When either n or l is sufficiently large the scale of spatial variation of the eigenfunction is much less than that of the basic state, and asymptotic methods can be used. To a first approximation the perturbation to the gravitational potential can be ignored (78). Since all the solar modes that have been observed and unambiguously identified fall into this category, it is useful to discuss the asymptotic properties in some detail.

The analysis can be carried out from two points of view. Either the separable form (Equation 3.1) can be substituted into the equations of motion, and the resulting ordinary differential equations solved by JWKB theory (293, 322). Alternatively, the three-dimensional equations can be approximated directly and the eigenfrequencies obtained as resonance conditions on integrals along ray paths (157, 160, 212, 261, 262). Examples of ray paths are shown in Figure 2. In both cases the equation determining the eigenfrequencies can be written in the form (95):

$$\frac{(n+\tilde{\alpha})\pi}{\omega} = \omega^{-1} \int_{r_1}^{r_2} \kappa dr \equiv \int_{r_1}^{r_2} \left[1 - \frac{\omega_L^2}{\omega^2} \left(1 - \frac{N^2}{\omega^2} \right) - \frac{\omega_c^2}{\omega^2} \right]^{1/2} \frac{d \ln r}{a}, \quad 3.2$$

where $\tilde{\alpha}$ is a constant of order unity, $a = c/r$ and $\omega_L = La$ is the Lamb frequency, with $L^2 = l(l+1)$ or $(l+1/2)^2$ depending on whether the spherical harmonic decomposition or ray theory is used. The quantity κ can be

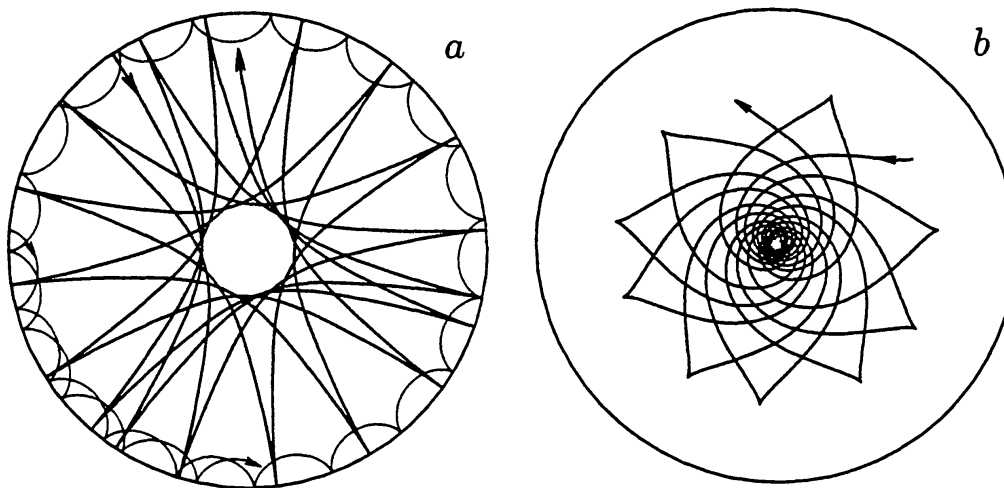


Figure 2 Ray paths in the standard model of the sun represented by the continuous line in Figure 1: (a) for two acoustic waves; the more deeply penetrating wave is p_8 ($l = 2$) and the shallower wave is p_8 ($l = 100$); (b) for the gravity wave g_{10} ($l = 5$). Note that the number of reflections per revolution is not integral, and indeed is almost never rational, so the ray paths are not closed.

regarded as the vertical component of the wave number characterizing the mode. The limits of integration r_1 and r_2 are radii at which κ vanishes and between which κ is real. They are the radii of the inner and outer caustic surfaces that form the envelopes of the rays (Figure 2), and between which the waves are trapped. Furthermore,

$$N^2 = g \left(\frac{1}{H} - \frac{g}{c^2} \right) \equiv \frac{gv}{r} \quad 3.3$$

is the square of the buoyancy frequency, g being the acceleration due to gravity, and ω_c is the acoustical cutoff frequency:

$$\omega_c^2 = \frac{c^2}{4H^2} \left(1 - 2 \frac{dH}{dr} \right), \quad 3.4$$

where H is the density scale height. Equations 3.3 define the dimensionless convective stability parameter v . Except in the convection zone (where generally N^2 is small and negative), N^2 and ω_c^2 are similar in magnitude; except near the surface, both are much less than the Lamb frequency ω_L , which is an approximate lower bound to the frequencies at which acoustic propagation can occur in the deep interior.

The phase constant $\tilde{\alpha}$ depends on conditions in the vicinity of the turning points r_1 and r_2 ; formally $\tilde{\alpha} = -1/2$ (71, 157), but in practice Equation 3.2 can be a more accurate representation if $\tilde{\alpha}$ is modified somewhat. For

example, the upper turning point r_2 for p modes is approximately the level at which $\omega_c = \omega$; here the wavelength of the oscillation is comparable with H , and the conditions under which the asymptotic expansion was assumed to have been carried out do not apply. Since the region where this occurs is quite shallow, the error introduced may be represented by an additional phase jump at the reflecting surface, which is equivalent to modifying $\tilde{\alpha}$. For high-order g modes the upper turning point is immediately beneath the base of the convection zone, where the gradient of N^2 changes abruptly. This near-discontinuity influences the eigenfunctions in the evanescent region, by modifying the conditions presented to the wave at $r = r_2$, thereby changing $\tilde{\alpha}$ as well (115, 116, 265, 310, 337). Finally, for low-degree modes that penetrate close to the center of the star, the influence of the singularity at $r = 0$ in the equations governing separable solutions [with $L^2 = l(l+1)$] also modifies $\tilde{\alpha}$; in principle there should be a corresponding contribution in the ray description [for which $L^2 = (l+1/2)^2$].

Equation 3.2 can be improved by taking into account the perturbation to the gravitational potential. This has been carried out, to different orders of approximation, by Vorontsov (324, 325), Tassoul (311), and Dziembowski & Gough (110).

The asymptotic form for the eigenfunctions away from the turning points r_i is given by

$$(\Xi, H) \sim \begin{cases} r^{-1}(\kappa/\rho)^{1/2}(\cos\psi, Lr^{-1}\kappa^{-1}\sin\psi) & r_1 < r < r_2 \\ r^{-1}(\kappa/4\rho)^{1/2}(1, Lr^{-1}\kappa^{-1})e^{-\psi} & r < r_1, r > r_2 \end{cases} \quad 3.5$$

for p modes, and

$$(\Xi, H) \sim \begin{cases} r^{-1}(\rho\kappa)^{-1/2}(\sin\psi, L^{-1}r\kappa\cos\psi) & r_1 < r < r_2 \\ r^{-1}(4\rho\kappa)^{-1/2}(1, L^{-1}r\kappa)e^{-\psi} & r < r_1, r > r_2 \end{cases} \quad 3.6$$

for g modes, where

$$\psi = \begin{cases} \int_{r_1}^r \kappa dr + \frac{\pi}{4} & r_1 < r < r_2 \\ \left| \int_{r_1}^r \kappa dr \right| & r < r_1, r > r_2 \end{cases} \quad 3.7$$

and in the evanescent region r_i is the turning point closest to r .

ACOUSTIC MODES When ω is high one might consider neglecting N^2/ω^2 and ω_c^2/ω^2 compared with unity, and approximating Equation 3.2 by

$$\frac{(n+\alpha)\pi}{\omega} \sim \int_{r_1}^{r_2} \left(1 - \frac{a^2}{w^2}\right)^{1/2} \frac{d\ln r}{a} \equiv F(w), \quad 3.8$$

where $w = \omega/L$. To be sure, the neglect of ω_c^2/ω^2 is a poor approximation near $r = r_2$ (where $\omega_c \simeq \omega$), but since this occurs in a relatively thin layer, its influence can be absorbed into $\tilde{\alpha}$, which we now replace by α . Indeed, if the stratification were that of a complete plane-parallel polytrope of index μ , the effect of neglecting ω_c is precisely just that, with $\alpha = \mu/2$ and r_2 being replaced by the radius R of the star. The sun is not a polytrope, however, so we admit the possibility of α being a function of ω . The integrand in Equation 3.2 depends only weakly on l near the surface of the star, where $\omega_L^2/\omega^2 \ll 1$, and therefore α and the eigenfunctions too can depend only weakly on l . We therefore ignore such dependence. Except when l is large, the radius of the lower turning point is given by

$$a(r_1) \simeq w. \quad 3.9$$

It is plotted in Figure 3 for three typical values of ω . It is evident from Equation 3.5 that $|\Xi| \gg |\mathbf{H}|$, except possibly near the turning points and, of course, near the nodes of Ξ . When $n \gg 1$ the motion is predominantly vertical even when l is quite large.

For low-degree modes with $n/l \gg 1$, the lower turning point r_1 is much less than R , and the eigenfrequency equation simplifies further to (157, 310)

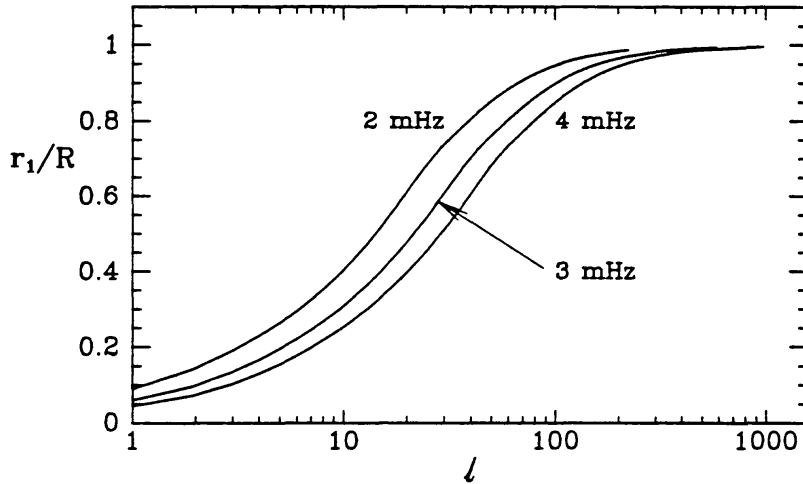


Figure 3 Lower turning points for p modes of a solar model, determined by the vanishing of κ , plotted against degree l for the three cyclic frequencies $\nu = \omega/2\pi = 2, 3, 4$ mHz. The curves for 2 and 3 mHz terminate at the lowest-order modes, at values of l determined by Equation 3.2 with $n = 1$.

$$\omega \sim \left(n + \frac{1}{2}l + \frac{1}{2}\mu + \frac{1}{4} \right) \omega_0 - (AL^2 - B)\omega_0^2/\omega, \quad 3.10$$

where μ is the effective polytropic index near $r = r_2$,

$$\omega_0 = \pi \left(\int_0^R c^{-1} dr \right)^{-1}, \quad 3.11$$

$$A = \frac{1}{2\pi\omega_0} \left[\frac{c(R)}{R} - \int_{r_1}^{r_2} \frac{dc}{dr} d\ln r \right] \quad 3.12$$

and

$$B = \frac{\omega^2}{\pi\omega_0} \int_{r_1}^{r_2} \left(1 - \frac{a^2}{w^2} \right)^{-1/2} \left[1 - \left(1 - \frac{\omega_c^2}{\omega^2} \right)^{1/2} \right] \frac{dr}{c}. \quad 3.13$$

The second of the two terms on the right-hand side of Equation 3.10 for ω is much smaller than the first; the first term in brackets in Equation 3.12 is much smaller than the second. The characteristic frequency ω_0 is a global quantity, and is a measure of the harmonic mean of the sound speed through the star; A has a comparatively sensitive dependence on conditions near the center of the star and B depends predominantly on conditions near the upper turning point r_2 (157). Tassoul (311) has recently extended Equation 3.10 to account for perturbations to the gravitational potential.

GRAVITY MODES For modes trapped beneath the convection zone, the approximation analogous to Equation 3.8 is

$$\frac{(n+\alpha_g)\pi}{L} \sim \int_{r_1}^{r_2} \left(\frac{N^2}{\omega^2} - 1 \right)^{1/2} d\ln r, \quad 3.14$$

for $r_1 \ll R$ and $r_2 \simeq r_c$, where r_c is the radius of the base of the convection zone. The phase constant α_g depends particularly on the stratification near $r = r_c$. Only modes with low l are of practical interest—high-degree modes cannot tunnel through the convection zone to be detectable in the photosphere (61, 111).

The ratio of the amplitudes of the vertical and horizontal components of the displacement is roughly $L/rk \sim l/n$ well away from the turning points: The motion is in the form of tall thin oscillating eddies when $l \gg n$, and short squat eddies when $n \gg l$.

Differential Kernels

Differential kernels measure the sensitivity of the eigenvalues to perturbations in the structure of the solar model. They are most directly

computed from the variational principle for adiabatic oscillations (48, 227), which we write formally as

$$I\omega_i^2 = \int_0^R G(\mathbf{S}, \xi_i; r) dr, \quad 3.15$$

where $\mathbf{i} = (n, l)$ labels the mode, and $\mathbf{S}(r)$ denotes the equilibrium structure of the sun. The quantity I is defined by

$$I = 4\pi \int_0^R \xi_i \cdot \dot{\xi}_i \rho r^2 dr; \quad 3.16$$

it is a measure of the inertia (or, alternatively, the energy) of the mode relative to an appropriate normalization of the eigenfunction ξ_i , which is usually set by specifying the radial component of the displacement (or, alternatively, the velocity) at $r = R$. From this one can derive a linear approximation to the change $\delta\omega_i^2$ in ω_i^2 resulting from a small variation $\delta\mathbf{S}(r)$ in \mathbf{S} . Because any eigenvalue ω_i^2 is determined as a stationary value of the ratio of the integrals in Equation 3.15 with respect to permitted variations $\delta\xi_i$ (i.e. those that do not violate the boundary conditions) in ξ_i , the result is independent of $\delta\xi_i$. Thus the variational formulation does not at this stage require the computation of the perturbed eigenfunctions. The perturbed frequency is therefore given by

$$\frac{\delta\omega_i^2}{\omega_i^2} = \int_0^R \mathbf{K}(\mathbf{S}, \xi_i; r) \cdot \delta\mathbf{S} dr \quad 3.17$$

where $\omega_i^2 \mathbf{K}$ is the variational gradient of G/I with respect to \mathbf{S} . It depends, of course, on the choice of the components of the function \mathbf{S} chosen to represent that equilibrium structure; it is a straightforward matter to transform from one set of components to another, by appropriate partial integrations of Equations 3.17 and the use of the hydrostatic equations that constrain \mathbf{S} (112, 160, 162, 167), though sometimes the outcome requires the solution of a differential equation. For p modes it is natural to use as variables $c^2 = \gamma p/\rho$, or more straightforwardly $u = p/\rho$, and perhaps the helium abundance Y on which the constitutive coefficient $\gamma = (\partial \ln p / \partial \ln \rho)_s$ depends with the thermodynamic derivative being taken at constant specific entropy s ; for g modes v most naturally replaces u . Thus in Figure 4 we display kernels for $\mathbf{S} = (\ln u, Y)$ and $\mathbf{S} = (\ln v, Y)$. One can see how p modes are most sensitive to the outer layers of the sun and g modes are most sensitive to the inner regions, as is also evident from the ray diagrams in Figure 2.

Kernels for high-degree p modes for variations in c^2 are illustrated in

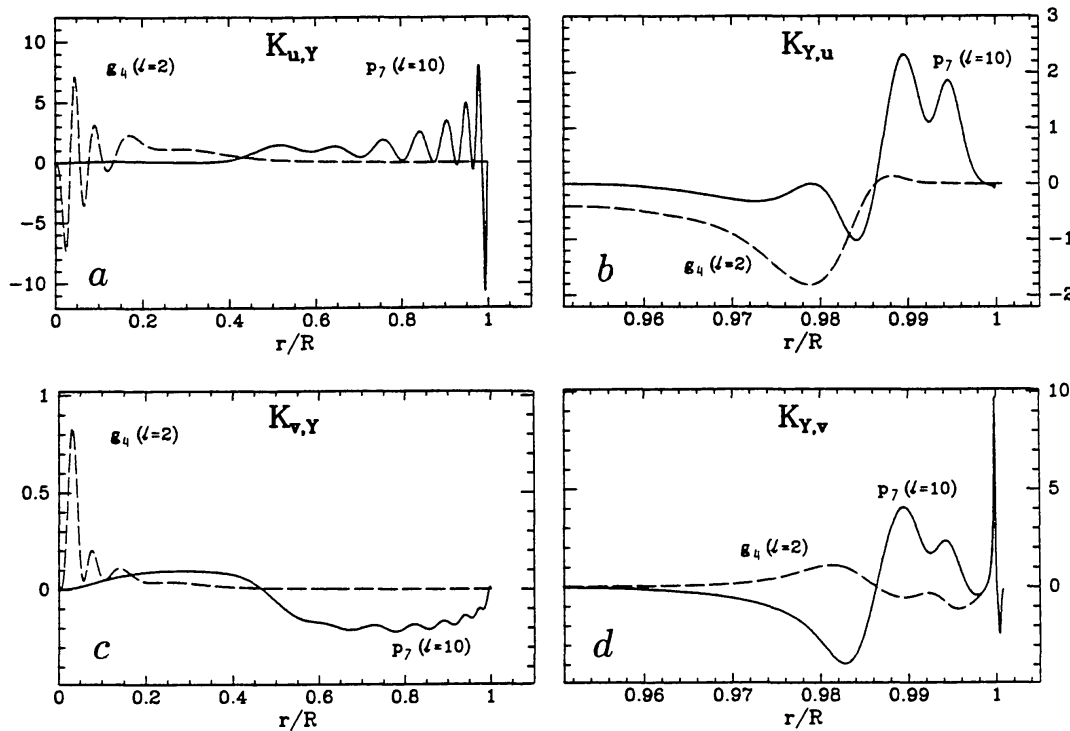


Figure 4 Differential kernels for hydrostatic stratification plotted against relative radius r/R for the modes p_7 ($l = 10$) and g_4 ($l = 2$): (a) $K_{u,Y}$ and (b) $K_{Y,u}$, where $u = p/\rho \propto c^2$, defined such that Equation 3.17 takes the form $\delta \ln \omega_i^2 = \int (K_{u,Y} \delta \ln u + K_{Y,u} \delta \ln Y) dr$, (c) $K_{v,Y}$ and (d) $K_{Y,v}$ defined analogously. The g -mode kernels have been scaled by factors 0.02, 10⁴, 0.005, and 2 in (a), (b), (c), and (d) respectively.

Gough & Toomre (168) for a plane-parallel polytropic stellar envelope. Gough (148) displayed a selection of density kernels for low-order p and g modes of a standard solar model, ρ and c^2 kernels for high-order p modes can be found in Gough & Kosovichev (161) and Gough & Thompson (167); the c^2 kernels are similar to the kernels $K_{u,Y}$ in Figure 4.

4. OBSERVATIONAL PRINCIPLES

Helioseismology has benefitted in the past seven years from major advances in instrumentation for measuring Doppler velocities and intensity fluctuations associated with solar oscillations. These matters are discussed in detail in recent reviews (39, 177, 178, 232). The greatest challenge to the observation of p modes has been to develop instruments that permit stable Doppler imaging of the entire solar disk. In contrast, the challenge in detecting g modes is to separate them from the solar convective motion and from the noise introduced by observing through the earth's atmosphere, which is particularly severe on the time scales characteristic

of g -mode periods. For all modes it is necessary to devise strategies to obtain observations of very long duration with as few gaps in the data as possible. Although it would be of great benefit to utilize g -mode data, especially in sampling the structure in the deep interior (154), at present there is uncertainty about whether these elusive modes have even been detected (127, 134, 182, 194, 266, 291). Therefore, we shall address here only the unambiguous advances (178) made in observing p modes and the new observing strategies now being implemented that should drastically broaden the data bases available for helioseismic inference.

Two basic observational techniques are used to study solar p modes, and these are accompanied by elaborate data-reduction procedures for deducing mode frequencies and lifetimes, and for estimating the amplitudes. The first involves measurement of Doppler shifts of a given spectral line, either in integrated sunlight (no imaging) using a very stable Doppler analyzer, by employing atomic resonance scattering by sodium or potassium (76, 117, 124, 137, 171, 206, 258), using one-dimensional imaging (employing a cylindrical lens to collapse the image onto a line) (98, 99), or with full two-dimensional imaging of the solar disk (44, 99a, 242, 270). The second approach is to measure brightness or intensity fluctuations, again either with or without imaging. That has the advantage of requiring simpler instruments, but appears to yield signals with a somewhat higher noise level than Doppler observations, largely because there are substantial intensity fluctuations associated with phenomena such as turbulent granulation in the surface layers. Brightness oscillations in integrated sunlight generated by low-degree p modes have been observed with precision from space using an active cavity radiometer (ACRIM) on the *SMM* satellite in near-earth orbit (334, 335), and with greater continuity using an irradiance photometer (IPHIR) operated during the cruise phase of the mission *Phobos* to Mars (129, 130). Ground-based observations of intensity fluctuations of intermediate- and high-degree modes using imaging detectors have been most effective with a narrow-bandpass filter centered on the deep Ca K spectral line (100, 102, 207, 208). These have permitted exceptional imaging observations from the South Pole over an extended interval of time with only few gaps in the data.

Two-dimensional Doppler imaging has been achieved with several types of rapidly tunable narrow-bandpass filters, each used to obtain successive solar images while varying the wavelength sampled in a spectral line, and then digitally combining the images to deduce the Doppler shifts. Oscillation measurements have thus been made with atomic resonance magneto-optical filters (267, 270), solid Michelson interferometers (37, 44, 180, 197), birefringent filters (191, 242), and Fabry-Perot étalons (192, 279). The data consist of a time series of Doppler images. These are

analyzed to isolate contributions from individual oscillation modes, accomplished typically by fitting each image to some large number of projected spherical harmonics and then Fourier transforming the coefficients to yield temporal power spectra (39). Such procedures have led to precise determinations of intermediate- and high-degree mode frequencies, including the degeneracy splitting (38, 44, 100, 233, 235, 239, 240, 271). The intermediate-degree modes have been measured with the greatest precision; their frequencies are plotted in Figure 5.

A major observational challenge is to obtain sufficiently long, nearly uninterrupted Doppler observations. To this end three worldwide networks of observing stations are working at achieving nearly continuous coverage, thereby reducing the deleterious effects of sidelobes in temporal power spectra. The first is the Global Oscillations Network Group (GONG) project, which is working to place at six different longitudes around the world identical Doppler imaging instruments using solid Michelson interferometers (180, 181, 185, 187, 188) to obtain good spatial resolution to study intermediate- and high-degree modes. Prototype observations are now proceeding, and the network is expected to be fully operational in 1993, and to operate for at least three years. Complementing the GONG data will be whole-disk Doppler observations from two inde-

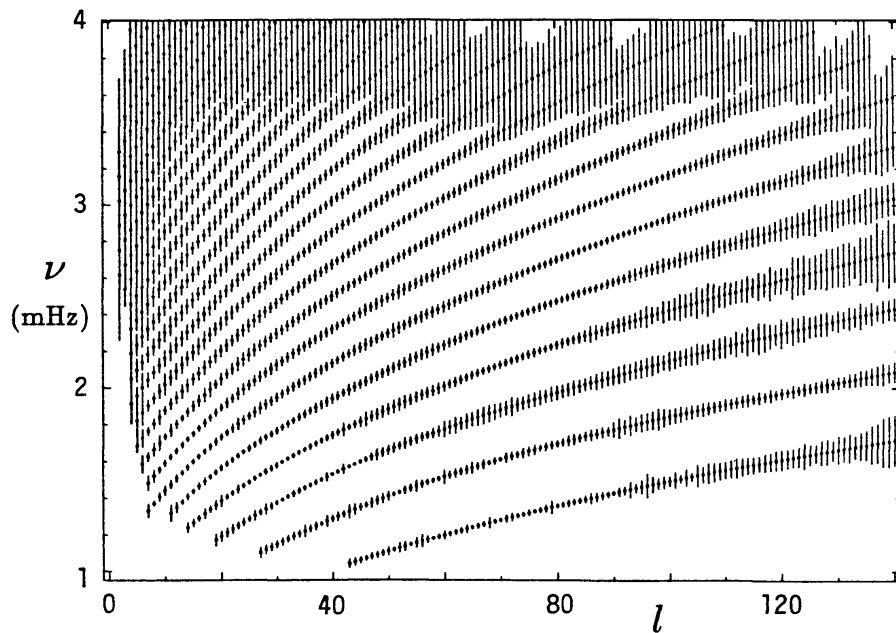


Figure 5 Solar p -mode frequencies measured by Libbrecht & Woodard (239, 240). The vertical lines represent $\pm 1000\sigma$ errors, where σ is a standard error. Sequences of frequencies of modes of fixed order n are approximately parabolic at high l ; the lowest-frequency sequence has $n = 1$.

pendent ground-based networks (118, 282) aimed at obtaining accurate frequencies of low-degree modes.

The data to be obtained from the ground must in turn be supplemented by observations carried out from space in order to have access to the very high-degree modes (l up to about 4000) needed to study detailed dynamics in the convection zone; seeing distortions from the ground already play havoc with l above 400 (189). These observations will be accomplished by the Solar Oscillations Investigation (SOI) employing a Michelson Doppler imaging instrument (197, 281) to be operated on the *SOHO* spacecraft. It is to be placed in a halo orbit about the L_1 Lagrangian point between the earth and the sun, chosen not only because it is thus in continuous sunlight, but also because it will have a low velocity relative to the sun. The complement of helioseismological experiments on *SOHO* also includes a spatially unresolved atomic resonance scattering instrument (GOLF) (82), and an active cavity radiometer coupled with photometers with limited spatial resolution (VIRGO) (128), both of which will study low-degree modes with particular emphasis on g modes. The *SOHO* spacecraft is expected to arrive on station in 1995 and to operate for at least three years.

5. INVERSION OF DATA

Reliable seismic information about the stratification of the sun has come entirely from five-minute p modes. The data have been analyzed in two separate ways: by model-fitting and by inversion. The first method is to construct a set of solar models with different values of one or more adjustable parameters of the theory and to find the values of those parameters yielding eigenfrequencies that best fit the observations. This was first carried out in an attempt to determine Y_o (65, 296), yielding values of about 0.25 and 0.23 respectively. The calibration suffers the deficiency of being dependent on all the assumptions and uncertainties of the theory of the evolution of the sun. These are surely significant: It has not been possible to find a model of the sun that reproduces the observations precisely. To understand what is wrong it is useful to plot against ω_i the scaled differences $I\delta\omega_i$ between the frequencies of the sun and model. By multiplying the differences by the modal inertia I one obtains a representation of the magnitude of the error in the restoring force responsible for the oscillations (52a, 159a). Since essentially all p modes with the same frequency look similar close to the surface of the sun, an error in the model near the surface would lead to a scaled frequency error that depends only on ω . The strong frequency dependence in Figure 6, in which only the l dependence of the inertia scaling has been included, therefore indicates that there is an error in the model near the surface. Indeed it follows from

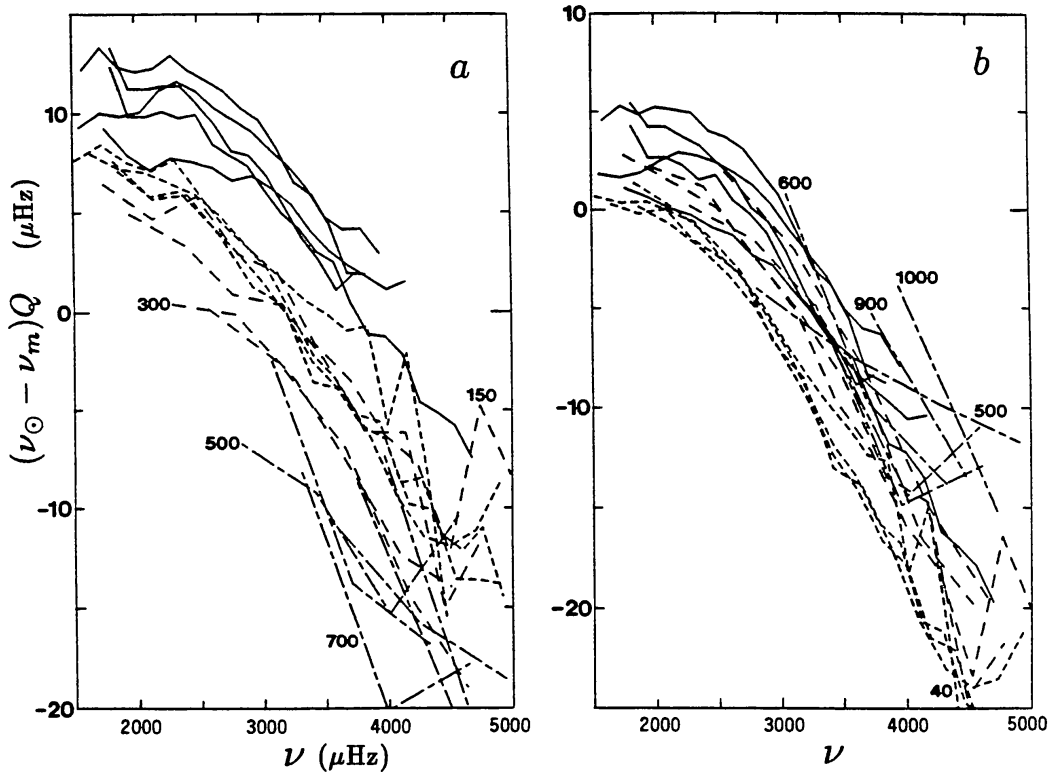


Figure 6 Scaled cyclic frequency differences $(\nu_{\odot} - \nu_m)Q$, where $Q = I(\nu, l)/\bar{I}(\nu)$ in which I is the inertia of the mode, and $\bar{I} = I(\nu, 0)$ is obtained by interpolation amongst the inertias of radial modes, ν_{\odot} is observed and ν_m is computed from a theoretical model: (a) ν_m computed with a relatively simple equation of state; (b) ν_m computed from the MHD equation of state. Points corresponding to a fixed value of l are connected by lines according to the following convention: solid, $l = 0, 5, 10, 20, 30$; short-dashed, $l = 40, 50, 70, 100$; long-dashed, $l = 150, 200, 300, 400$; alternating short- and long-dashed, $l = 500, 600, 700, 800, 900, 1000$; the labels on the diagram denote values of l [from (53)].

the structure of Equation 3.15 that if the only error were actually in the very surface layers, where ξ_i is normalized, then the right-hand side would be essentially independent of the mode: $I\omega_i^2$ would be approximately constant (as it is for the solar-cycle frequency changes discussed in Section 10). Notice that in Figure 6b much of the dependence on l has been removed by introducing the MHD equation of state (200, 252), which implies that much of the error well beneath the surface layers has been eliminated. Further discussion is provided by Christensen-Dalsgaard (52a, 53).

To acquire more precise information about the nature of the errors in the model it is expedient also to use inverse techniques, which aim at extracting those aspects of the structure of the sun that are genuinely determined by the data. These techniques require solutions of the forward problem, but we defer discussion of those to subsequent sections. We first

summarize inversion methods that have been used, and discuss what has been learned from them.

Direct Asymptotic Determination of the Sound Speed

The starting point of our discussion is the approximate asymptotic expression given by Equation 3.8. It is sufficiently simple that it can be inverted analytically, yielding (152)

$$r = R \exp \left\{ \frac{-2}{\pi} \int_{a_s}^a (w^{-2} - a^{-2})^{-1/2} \frac{dF}{dw} dw \right\}, \quad 5.1$$

where $a_s = a(R)$. Strictly speaking, the integral should be a sum over the discrete values of w , but it is more convenient to regard F as a smooth function of the continuous variable w . The equation determines the radius at which $w = a \equiv c/r$, from which it is straightforward to obtain $c(r)$.

In view of the special structure of Equation 3.8, both F and α can be determined from the data simply by demanding that they be functions of only w and ω respectively. Of course a perfect fit cannot be achieved, even if there were no errors in the data, because the equation is not exact. Nevertheless, it has been found to be extremely useful by virtue of its simplicity. Moreover, the information it provides is independent of any theoretical solar model, and therefore its validity does not rest on assumptions such as those listed in Section 2, save that of hydrostatic support.

Equation 5.1 has been used to estimate $c(r)$ in the sun by Christensen-Dalsgaard et al (60), using data obtained by Duvall & Harvey (96, 98, 179). They assumed α to be constant, as had Duvall (96) previously, and eliminated some of the systematic errors in the inversion by also inverting theoretical eigenfrequencies of a standard solar model (49) and taking the difference between the two inversions as an estimate of the difference between the sound speed in the sun and that in the model. The results appeared to be accurate to about $\frac{1}{2}\%$ for $r > 0.3R$, except very near the surface. They indicated that the theoretical model accurately reproduced the solar sound speed for $r \gtrsim 0.5R$, except possibly near the surface where the inversion failed. But in the $0.3R$ to $0.5R$ range the sound speed in the sun was found to be some 1% greater than in the model. Permitting a frequency variation of α takes some cognizance of the neglected ω_c , and improves the accuracy of Equation 5.1 (32, 33, 156).

In practice it is not possible to evaluate the integral in Equation 5.1 completely because modes do not exist with w close to a_s . Consequently it is necessary to make an estimate of F at low w , which is tantamount to assuming a structure for the outer layers of the sun. Any error in this estimate can be regarded as a scaling error in the inferred value of r . That

this may be large has caused some concern (318). However, it has been demonstrated that at depths substantially greater than the lower turning point of the least deeply penetrating mode, that error is likely to be quite small; for example, it was found to be possible to determine the depths of the convection zones of three similar solar models to within $0.005R$ (69, 156).

Additional improvements in the inversion can be achieved by taking further account of the neglected terms in Equation 3.2. This can be achieved by regarding the neglected terms as a small perturbation and expanding the integral in Equation 3.2 about that in Equation 3.8, retaining only the linear terms (152). This adds the term $\omega^{-2}\Psi(w)$ to the left-hand side of Equation 3.8, where

$$\Psi \simeq \frac{1}{2} \int_{r_1}^{r_2} \left(\omega_c^2 - \frac{a^2 N^2}{w^2} \right) \left(1 - \frac{a^2}{w^2} \right)^{-1/2} \frac{d \ln r}{a}. \quad 5.2$$

Once again, by using the special functional form of the equation, $F(w)$, together with $\Psi(w)$ and $\alpha(\omega)$, can be determined (32, 33, 215).

One might expect that once $a(r)$ has been determined, the knowledge of $\Psi(w)$ could in principle be used to invert Equation 5.2 to obtain, with the help of the equations of hydrostatic support, ω_c^2 and N^2 . That is a difficult procedure, partly because $\Psi(w)$ is determined inaccurately from the small deviations of the frequencies from the asymptotic law (Equation 3.5). Moreover, Ψ is also influenced by perturbations in the gravitational potential (110, 324, 325), which we have ignored in this discussion.

An alternative procedure for inverting Equation 3.2 has been proposed by Shibahashi (294), and developed by Shibahashi & Sekii (289, 298). Rather than regarding the right-hand side as a function principally of w for each value of l , it is regarded as a function of n , which is considered to be continuous. The equation can then be inverted, in the manner that Equation 5.1 was derived, to provide $\omega^2 - c^2\kappa^2$, which Shibahashi calls the acoustic potential. It is determined as a function of the acoustic distance (sound travel time) between r_1 and r_2 . By using the fact that r_2 is only weakly dependent on l and that the difference between $\omega^2 - c^2\kappa^2$ and the square of the Lamb frequency is small, it is then a simple matter formally to determine da/dr from the l dependence of $\omega^2 - c^2\kappa^2$, and thence to determine $c(r)$. Once again, the small difference between the acoustic potential and ω_L^2 , and consequently ω_c^2 and N^2 , can in principle be determined once $a(r)$ is known.

Perturbation About a Solar Model

As an alternative to subtracting similar asymptotic inversions of solar and theoretical frequencies for the purposes of reducing systematic errors, the

eigenfrequency equation (3.8) can instead be perturbed and linearized in the differences between the sun and the model. The outcome is again invertible, and appears to be more stable than the direct method (68). (An inversion of the solar data is depicted in Figure 8.)

The most obvious deficiency of asymptotic procedures is their lack of precision. To obtain the most from the data it is evidently necessary to use the full oscillation equations, without unnecessary approximation. The object is to find a suitable structure $\mathbf{S}(r)$ that is consistent with the constraints represented by Equation 3.15. This is a nonlinear problem, which is to be solved by a sequence of linear iterations.

The procedure is to start from a trial structure $\mathbf{S}_o(r)$, computing the eigenfunctions ξ_{oi} and eigenfrequencies ω_{oi} , and then estimating the error $\delta\mathbf{S} = \mathbf{S} - \mathbf{S}_o$ in the trial from Equation 3.17 with $\delta\omega_i^2 = \omega_i^2 - \omega_{oi}^2$ and with \mathbf{S} , ω_i^2 and ξ_i replaced by \mathbf{S}_o , ω_{oi}^2 and ξ_{oi} . In principle the process can be repeated until it converges.

The problem of obtaining an approximate solution $\delta\mathbf{S}$ to linear integral equations of the type (3.17) is encountered in many branches of science. Geophysicists, in particular Backus & Gilbert (5–7), have pioneered this subject. We present here only a very brief summary because the application of inverse methods to helioseismology has recently been discussed elsewhere (74, 154, 313).

One of the most common approaches is to express $\delta\mathbf{S}(r)$ as a linear combination of basis functions $\psi_k(r)$:

$$\delta\mathbf{S} = \sum_k \alpha_k \psi_k. \quad 5.3$$

Because there are only a finite number of constraints (3.17), the function \mathbf{S} cannot be determined uniquely. The chosen set of basis functions must therefore be finite, and it is clear that the solution depends on that choice. The coefficients α_k must be chosen so that the representation (Equation 5.3) essentially reproduces the data. One does not need to satisfy the constraints (Equation 3.17) exactly because these data contain errors; indeed, one does not actually wish to do so because those errors would normally generate spurious solutions that have little or no resemblance to the true functions $\delta\mathbf{S}$. Therefore a compromise is reached, typically by minimizing

$$E \equiv \sum_i \sigma_i^{-2} \left[\frac{\delta\omega_i^2}{\omega_i^2} - \sum_k \alpha_k \int_0^R \mathbf{K}_i \cdot \psi_k dr \right]^2, \quad 5.4$$

where $\mathbf{K}_i = \mathbf{K}(\mathbf{S}_o, \xi_i; r)$ and σ_i^2 is the estimated variance of the probable error in the datum $\delta\omega_i^2$, subject to some additional constraint \mathcal{C} based on

smoothness or stability designed to restrain the influence of the errors. (For simplicity we are assuming the errors in the data to be independent.)

Backus & Gilbert (5) have argued that the most natural basis is a set of orthogonal functions constructed as linear combinations of the differential kernels \mathbf{K}_i . The choice is particularly advantageous for coping with the inevitable errors in the data, for there is a natural way of discarding members of the basis whose coefficients cannot be determined with sufficient precision from the data. This truncates the representation (Equation 5.3). The procedure is known as *spectral expansion*. One of its evident virtues is its mathematical elegance, particularly because it formally restricts possible “solutions” to lie only in the function space that can influence the data. However, the true merit should be judged by how well it can estimate the function $\delta\mathbf{S}$.

An alternative approach is to choose some arbitrary basis on the grounds of computational or conceptual convenience. A common procedure is to dissect the range $(0, R)$ of r into a set of contiguous intervals $\mathcal{J}_n = (r_{n-1}, r_n)$, $n = 0, 1, 2, \dots, N$, with $r_0 = 0$ and $r_N = R$, and take ψ_k to be linear, perhaps constant, in \mathcal{J}_k and zero elsewhere; an alternative is to select cubic splines in each interval. Such a set is orthogonal. In the case when ψ_k is constant in \mathcal{J}_k , the constraint \mathcal{C} might then be that a norm such as

$$D = 4 \sum_{n=1}^{N-1} (r_{n+1} - r_{n-1})^{-4} |\psi_{n-1} - 2\psi_n + \psi_{n+1}|^2 \quad 5.5$$

of the second differences (or in terms of some more precise estimate of the second derivative with respect to either r or the acoustical radius $\int c^{-1} dr$) be constrained. In practice this is achieved by minimizing $E + \lambda D$ for some value of the *tradeoff parameter* λ , which is chosen on the basis of an estimate of the influence of the errors in the data.

One of the properties of the data one might naturally wish to know is their ability to provide localized information about the function $\delta\mathbf{S}$. If the basis ψ_k is well defined, with no undetermined parameters, the minimization of E , or $E + \lambda D$, requires the solution of a set of inhomogeneous linear equations for the coefficients α_k , resulting in a representation (Equation 5.3) whose value $\overline{\delta\mathbf{S}}(r_0)$ at any point r_0 is a linear combination of the data:

$$\overline{\delta\mathbf{S}}(r_0) = \sum_i \beta_i(r_0) \omega_i^{-2} \delta\omega_i^2 = \int_0^R \sum_i \beta_i \mathbf{K}_i \cdot \delta\mathbf{S} dr \equiv \int_0^R \mathbf{A} \cdot \delta\mathbf{S} dr. \quad 5.6$$

Thus the inversion is an integral of the true function $\delta\mathbf{S}$, weighted with a

known averaging kernel $\mathbf{A}(r_0, r)$. The extent to which the data exhibit localized information in the inversion can be assessed simply by inspecting the kernels \mathbf{A} .

How localized can that kernel be? Backus & Gilbert (6, 7) provided a means of answering this question by seeking those coefficients β_i that make $\mathbf{A}(r_0, r)$ look most like the delta function $\delta(r - r_0)$, rather than minimizing E ; once again a constraint \mathcal{C} moderated by a tradeoff parameter must be added to ensure that the contamination of the average (Equation 5.6) by errors in the data is not too great. This procedure has become known as optimal averaging. Some examples of the optimal kernels \mathbf{A} are illustrated in Figure 7.

Testing Inversions

The ability of an inversion method to provide a useful representation of the system under investigation depends upon the forms of the kernels associated with the available data. Therefore the geophysicists' results cannot be applied uncritically to the sun, though of course the extensive experience of geophysicists has been useful for understanding the characteristics of the procedures.

Several tests have been carried out (66, 74, 154, 169), mainly on the simple scalar problem of determining the angular velocity $\Omega(r)$ of the sun (presumed independent of latitude) from artificial rotational splitting data

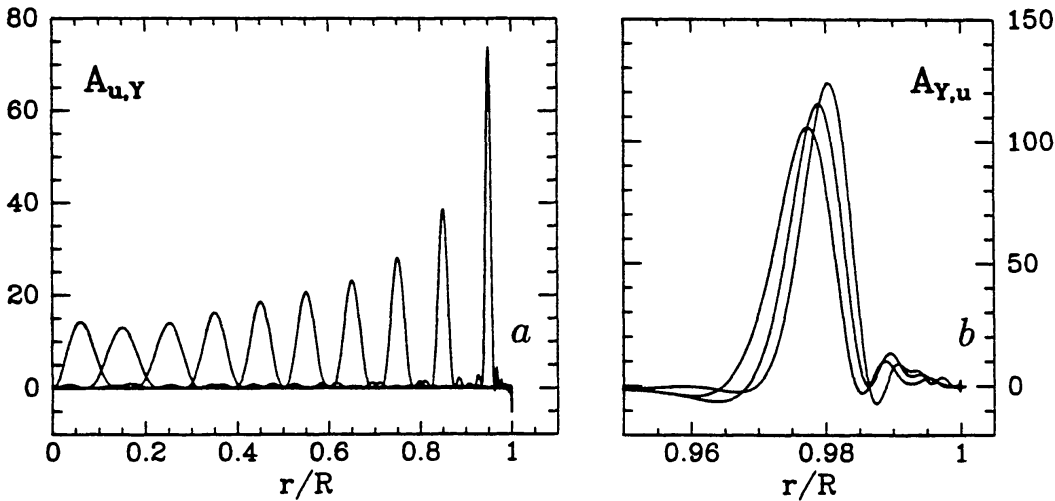


Figure 7 Optimal averaging kernels $A_{u,Y}$ and $A_{Y,u}$, defined by Equation 5.6 for $\delta S = (\ln u, Y)$, constructed in the manner of Backus & Gilbert (6, 7) from p -mode data kernels $K_{u,Y}$ and $K_{Y,u}$ such as those illustrated in Figure 4: (a) optimal u kernels, (b) optimal Y kernels. The Y kernels are large only in regions of ionization of abundant elements, and therefore it is only in those regions that optimal kernels $A_{Y,u}$ can be localized. The modes used in the combination (5.6) are those used for the inversions illustrated in Figure 8.

$\Delta\omega_i$. The constraints on Ω provided by the data are of the form (cf Equation 8.1)

$$\Delta\omega_i = \int_0^R K_i(r)\Omega(r) dr. \quad 5.7$$

One first invents a function $\Omega(r)$ and computes $\Delta\omega_i$ from Equation 5.7, the kernels K_i having been computed from Equation 8.1 using the eigenfunctions of a solar model. Then one attempts to recover $\Omega(r)$ by inverting the data $\Delta\omega_i$, perhaps after having added some noise to $\Delta\omega_i$. The kernels K_i correspond either to modes that have already been observed on the sun or to modes one might realistically hope to observe in the near future.

Recently a test of this kind has been carried out by some of the participants in GONG, using a variety of methods. The general conclusion was that when trying to infer $\Omega(r)$ over the entire range $(0, R)$ of r , both the expansion (Equation 5.3) with ψ_k being piecewise constant functions and the optimal averaging procedure performed well, but that the spectral expansion was apt to give poorer results (169). An excellent systematic comparison of some of the methods has been presented recently (74).

The oscillation frequencies must certainly be computed to a precision at least as high as that of the observations. To this end numerical schemes for computing both the equilibrium models and the oscillations need to be improved (54, 132, 133, 254).

6. INFERENCE OF HYDROSTATIC STRUCTURE

The Direct Outcome of Inversion

Both asymptotic methods and the potentially more accurate inversions of the full constraints (Equation 3.15) have their place. The asymptotic formulae are simple to evaluate, and thus can provide a convenient means of anticipating the results of the more cumbersome and hopefully more accurate procedures. Moreover, they provide considerable insight into how different combinations of the data are indices of certain aspects of the structure of the sun. One example is the small frequency separation $\omega_{n,l} - \omega_{n-1,l+2}$ which, as we discuss later, is influenced by chemical inhomogeneity in the core and thus provides some measure of the age of the sun. Another example comes directly from the realization that the frequencies of p modes are determined principally by the sound speed; ω_c^2 and N^2 induce quite small departures of the frequencies from the simple asymptotic pattern, and therefore their determination is extremely sensitive to errors in the data. To improve the accuracy requires the use of some g modes (154), whose frequencies depend directly on N^2 .

A strength of the inversion procedures described in the previous sections is that the results are independent of many of the assumptions of the theory of solar evolution. They demand solely that the sun be essentially in hydrostatic equilibrium, which is evident from the fact that the sun does not change substantially on a dynamical time scale. As with any inversion of dynamical oscillation frequencies, provided the oscillatory motion can be safely considered to be adiabatic, the outcome is a relation between pressure p and inertia (i.e. mass) density ρ , connected by the adiabatic exponent γ which enters the constitutive relation between their perturbations. There is a small additional dependence of the (gravitational) mass density ρ , neglected in the asymptotic discussion above, but considered to have been included in the constraints (Equation 3.15), which results from the perturbation induced in the gravitational potential. With a knowledge of say $c(r)$ and $\gamma(r)$, the equation of hydrostatic support

$$\frac{dp}{dr} = -\frac{Gm\rho}{r^2}, \quad 6.1$$

where G is the gravitational constant and

$$\frac{dm}{dr} = 4\pi r^2 \rho, \quad 6.2$$

can be integrated to determine $p(r)$ and $\rho(r)$. This is the direct product of helioseismic inversion.

Figure 8 illustrates some results of recent inversions. Shown are inferences of the relative differences in $u = p/\rho$ and ρ between the sun and a standard solar model. One of the striking features of the inversion is that p/ρ is greater in the radiative region $0.3 \lesssim r/R \lesssim 0.7$ of the sun than it is in the model. This is a robust feature of all inversions. It has been attributed to a deficiency in the opacity used for the reference model immediately beneath the convection zone (55, 60, 79, 80, 214). It is interesting that such an error has subsequently been found by recent opacity calculations at Livermore (202, 202a). The behavior of u in the energy-generating core is less certain because the contribution from the high-temperature core to the acoustic eigenfrequencies is quite small (see Figures 2 and 4). Figure 9 illustrates the degree to which the inversion has successfully reproduced the observed frequencies.

Helium Abundance and the Equation of State

To determine any subsidiary quantity, such as temperature, must require the use of information that cannot be determined by seismic analysis alone. In general, knowledge of p and ρ implies a relation between temperature

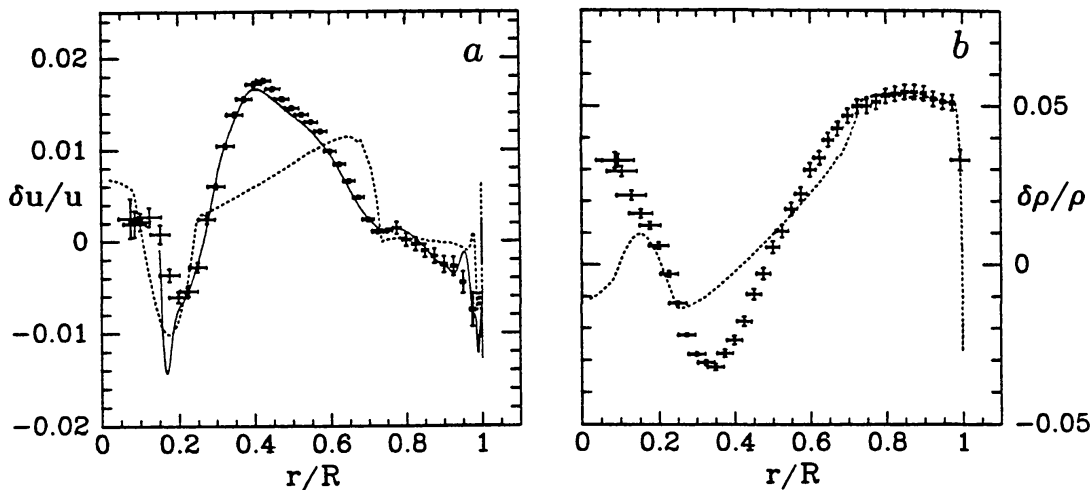


Figure 8 Relative differences $\delta u/u$ and $\delta \rho/\rho$ in $u = p/\rho$ and ρ between the sun and a standard solar model, where $\delta u = u_{\odot} - u_{\text{model}}$. The inversions are optimal averages of frequency data between 1.5 and 3 mHz obtained in 1986 by Libbrecht et al (241) and temporally-averaged data reported by Elsworth et al (119) adjusted to 1986 for solar-cycle variations, assuming a structural variation near the solar surface consistent with the frequency variations reported by Libbrecht & Woodard (239, 240) discussed in Section 10. The *vertical lines* represent standard errors; the *horizontal lines* the characteristic widths of the averaging kernels, some of which are illustrated in Figure 7. The *continuous curve* is an asymptotic estimate of $\delta c^2/c^2$ obtained by the differential method described in (68). The *dotted curves* illustrate a model with an internally mixed core, after (215a). The reference solar model is Model 2 of Christensen-Dalsgaard et al (68).

T and chemical composition \mathbf{X} , granted that the equation of state is known, but it cannot determine T and \mathbf{X} separately.

The most secure supplementary constraint that can be imposed is that, except from in the comparatively thin boundary layers, the convection zone is quite accurately adiabatically stratified. Although the mixing-length prescriptions used to model stellar convection zones are unreliable, their purpose is solely to provide a procedure whereby the stratification in the boundary layers can be computed (170). Adiabatic stratification in the interior of a zone with high Rayleigh number, such as in the sun, is a property not only of mixing-length models, but also of all more sophisticated theories and of all known instances of real (e.g. laboratory) convection.

One can draw interesting conclusions even if only the sound speed $c(r)$ is reliably determined seismologically. Together with the adiabatic and hydrostatic constraints it implies that (153)

$$W(r) \equiv \frac{r^2}{Gm} \frac{dc^2}{dr} = \frac{1 - \gamma_p - \gamma}{1 - \gamma_{c^2}} = 1 - \gamma \left[1 + \left(\frac{\partial \ln \gamma}{\partial \ln p} \right)_s \right] \equiv \Theta(r), \quad 6.3$$

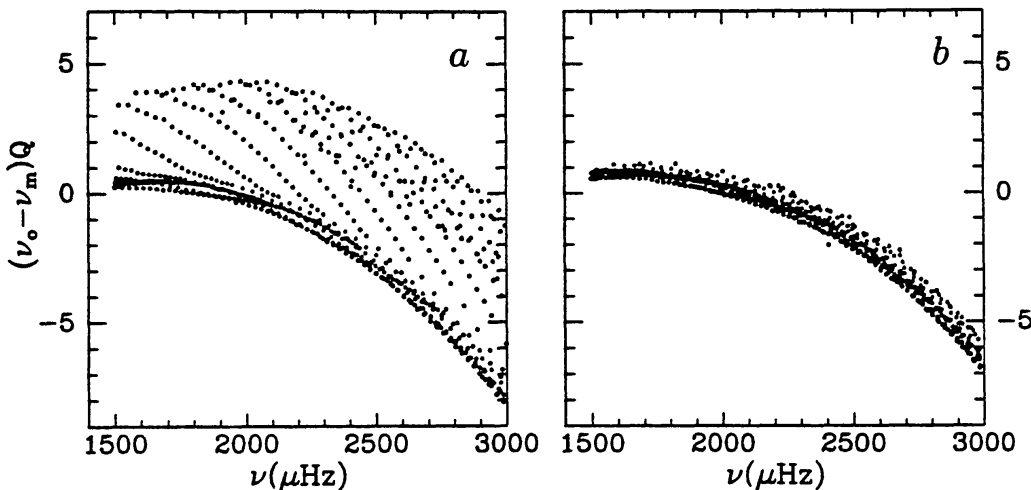


Figure 9 (a) Differences between the observed solar frequencies used in the inversion illustrated in Figure 8 and the eigenfrequencies of the reference model, scaled with normalized modal inertia as in Figure 6, and plotted against cyclic frequency. (b) Similarly, differences between the observed solar frequencies and those implied by $\delta u/u$ and $\delta \rho/\rho$ depicted in Figure 8, plotted on the same scale as (a). The removal of the l dependence by the inversion, resulting in scaled errors that are essentially a function of frequency alone, indicates that the predominant remaining errors are near the surface of the sun. The units are μHz .

where γ_ρ and γ_{c^2} are the partial logarithmic derivatives of γ with respect to ρ and c^2 at constant c^2 and ρ respectively, and s is specific entropy. The left-hand side of Equation 6.3 is determined by the hydrostatic stratification $p(r)$, $\rho(r)$, $c^2(r)$; the right-hand side is a pure thermodynamic quantity. For a perfect monatomic gas $\Theta = -2/3$, but when the gas is in a state of partial ionization Θ departs from that value. Therefore Θ measures the influence of ionization on γ , and its magnitude evidently depends on the abundance of the ionizing element. This is illustrated in Figure 10 where Θ and W are plotted for two models of the solar envelope. The most promising region to investigate is the He II ionization zone because it is isolated from the He I and H ionization zones and is sufficiently deep in the convection zone for adiabatic stratification, which renders $W = \Theta$.

It appears from Figure 10 that given a sufficiently accurate seismic determination of W , it should be possible to measure the helium abundance in the convection zone (86). Given no macroscopic material mixing with the products of the nuclear reactions in the core, no substantial gravitational settling, nor contamination by material accreted by the sun, this helium abundance then is the zero-age main-sequence abundance Y_0 . The measurement is not easy, however, partly because it depends on the derivative of c^2 with respect to r , which itself is already determined in the

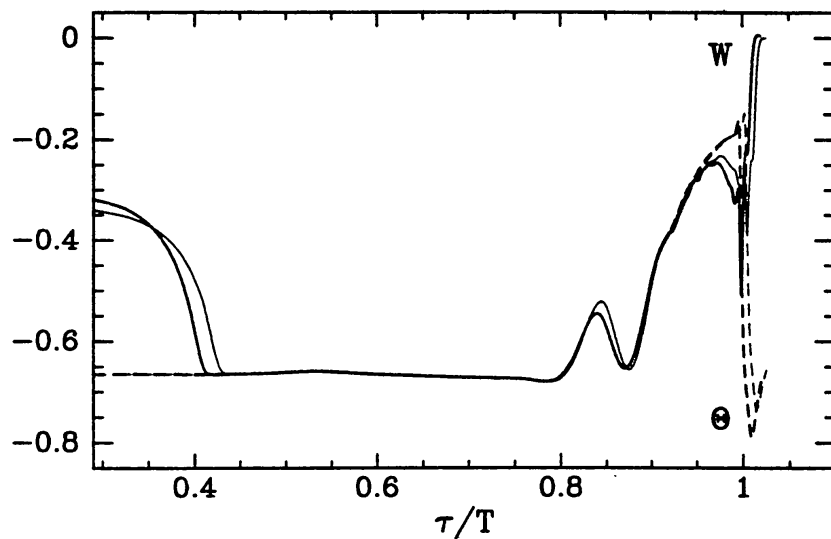


Figure 10 The functions W and Θ , defined by Equation 6.3, from two models of the sun, plotted against relative acoustic radius τ/T , where $\tau(r) = \int_0^r c^{-1} dr$ and $T = \tau(R)$. The thick curve was computed from Model 2 of Christensen-Dalsgaard et al (68), having $Y_0 = 0.237$, the thin curve from Model 4, having $Y_0 = 0.274$. Throughout the adiabatically stratified region of the convection zone, $W = \Theta$, and the outside regions of ionization of abundant elements, $\Theta \approx -2/3$; the small deviations from that constant value deep in the convection zone result from the partial ionization of oxygen and iron. The sharp divergence of W from Θ at $\tau/T \approx 0.4$ marks the base of the convection zone. The peak near $\tau/T = 0.83$ results from He II ionization.

asymptotic case via Equation 5.1 in terms of a derivative dF/dw of the data (and by the other methods must therefore also be determined in terms of some similar error-enhancing combination of data). It is also quite dependent on the equation of state, which is not accurately known. Indeed, subtleties in the shape of the inferred function $\Theta(r)$ may provide important diagnostics for theories of the equation of state. A reliable determination of Y_0 by this method has not yet been accomplished (88), partly because of suspected inconsistencies and errors in the high-degree data upon which it depends, and partly because of uncertainties in our knowledge of $\gamma(c^2, \rho, X)$.

Recently a very accurate set of frequencies of modes with $4 \leq l \leq 140$ (see Figure 5) has been obtained by Libbrecht and his colleagues (236, 241). Evidently, these too depend on W . However, because the lower turning points of all the modes lie well below the He II ionization zone (159a), the dependence on l is weak and a reliable determination of W from these modes alone is not possible. Nevertheless, an integrated effect of γ variations has been obtained from inversions by optimal averaging (87) and by minimizing a measure similar to E , defined by Equation 5.4, of frequency mismatch (113). The results are rather different: $Y_0 = 0.268$ and 0.234 respectively, each with a formal uncertainty of about 0.01, which

may have resulted from the use of different subsets of the data. Model calibrations based on the asymptotic phase factor $\alpha(\omega)$ occurring in Equation 3.8 have yielded $Y \simeq 0.25$ (72, 326). Recent unpublished collaborative work by Däppen and coworkers and Dziembowski's group (see also 87, 113) have isolated the major uncertainties: one is in the equation of state, different versions of which were used in the independent inversions; the other appears to have resulted from apparent inconsistencies in the data, which could have arisen from measurement errors but which might be a product of errors in the physical assumptions used in computing the oscillation eigenfrequencies.

An accurate measurement of the shape of the function W in the He II ionization zone could provide an important test of the equation of state. At present, however, we must be content with a direct comparison of raw frequencies (53, 56, 58) (see Figure 6). This suggests that the most accurate equation of state currently available for stellar modeling is probably either that developed by Mihalas, Hummer & Däppen (200, 252), or that developed at Livermore (203, 273)—the small differences between which are not yet understood (84, 89). The theories that produce those equations are complicated, taking into account many small details of atomic transitions that probably have little dynamical influence, though they are of considerable importance to the subsequent computation of opacity, which is now under way. Those aspects of the theory that are critical to the equation of state are yet to be isolated.

Depth of the Convection Zone

The radiative interior of the sun is not adiabatically stratified, and there Equation 6.3 does not hold. The thermodynamical quantity Θ remains close to $-2/3$, but W rises abruptly beneath the base of the convection zone. This property is evident in Figure 10, and can be used to measure the depth of the base of the convection zone. Indeed, the sharp change in curvature of c^2 is also clearly visible in Figure 1, and was seen in the first c^2 inversions of solar data (60) to occur in the vicinity of $r/R = 0.7$. More recent inversions by Vorontsov & Zharkov (327) to obtain W are consistent with this finding.

Using W as a diagnostic, Christensen-Dalsgaard et al (69) have recently determined the depth of the convection zone to be $0.287 \pm 0.003R$ beneath the photosphere. This result is consistent with an earlier calibration of a theoretical model of the solar envelope (21) using frequencies of modes that do not penetrate to the base of the zone. In principle a careful analysis of the manner in which W rises in the radiative interior can provide information about possible overshooting of convection or of the existence of concentrated magnetic fields near the convective-radiative interface such

as have been suggested in connection with the solar cycle (283, 302, 322a). Such analysis has not yet been carried out.

Mixing and the Solar Age

The depression in c^2 at the center of the sun evident in Figure 1 results from the augmentation of the molecular weight μ by the ${}^4\text{He}$ produced by the nuclear reactions. Thus the magnitude of the depression is an indicator of the sun's age. Indeed, if the standard model of the sun's evolution were correct, the age could be measured to within 3×10^8 y (164). In that case one could calibrate the model using precisely computed eigenfrequencies. The calibration can be carried out quite simply using the scaled frequency separation

$$d_{n,l} \equiv \frac{3v_{n,l}}{(2l+3)\bar{v}}(v_{n,l} - v_{n-1,l+2}), \quad 6.4$$

where $v_{n,l} = \omega_{n,l}/2\pi$ is cyclic frequency, coupled with the frequency interval

$$\Delta_{n,l} = v_{n,l} - v_{n-1,l} \quad 6.5$$

of low-degree five-minute modes. Here, the scaling factor \bar{v} is a representative value of $v_{n,l}$, and is included to make $d_{n,l}$ numerically similar to $v_{n,0} - v_{n-1,2}$. The use of $d_{n,l}$ is suggested by the asymptotic formulae (Equations 3.10–3.13), which imply that $d_{n,l} \propto A$ and is only weakly dependent on n . It is thus quite sensitive to conditions in the core and, being essentially independent of B , is relatively insensitive to the uncertain superficial layers of the sun. It is also an interesting diagnostic to investigate because in principle it can be measured in other stars.

It must be appreciated that the calibration is at present misleadingly optimistic, for it would be meaningful only if it were certain that the standard model were correct. The failure of the model to reproduce the observed frequencies is certainly indicative that something is wrong. Moreover, any modification to the model motivated merely by the desire to bring its eigenfrequencies into agreement with available observations, such as an increase in opacity in the radiative interior, cannot be regarded as securing a reliable model. It is therefore very difficult at present to assess how tightly estimates of the sun's age can be constrained.

It is noteworthy that any material mixing process in the core would smooth the helium distribution. The variation of c^2 observed in the sun certainly indicates that widespread mixing has not taken place. In particular, diffusive mixing increases $d_{n,l}$ beyond the limits set by observation; this is caused by a substantial augmentation of the sound speed in the central regions of the sun, which is associated with a diminution of the central

density (51, 52a) that is not consistent with Figure 8. However, present analysis cannot rule out local mixing within the core.

According to Equation 3.12, $A \propto d_{n,l}$ is an average of dc/dr weighted preferentially in the vicinity of the inner turning point r_1 . A negative gradient of μ decreases dc/dr and therefore increases A , and consequently $d_{n,l}$ (150, 264). Hence $d_{n,l}$ is expected to decrease with time (52). Any diffusive mixing of the chemical composition by fluid motion acts against the evolutionary tendency to enhance inhomogeneity, and is therefore almost bound to cause us to underestimate the sun's age. However, the most recent measurements of $d_{n,l}$ are in good agreement with standard theoretical predictions (117, 137a). Simply interpreted, this indicates negligible diffusion and a correct estimate of the sun's age. The influence of large-scale laminar advection has not been investigated in detail.

The Surface Layers

The greatest helioseismological uncertainties lie in the superficial layers of the sun. This is true for both the equilibrium structure and the oscillations. It is impossible to construct a reliable theoretical equilibrium model of those layers because the structure of any model must depend on the convective transport of heat and momentum—a trustworthy theory for which we do not have. Moreover, the physics of the oscillations is also poorly understood. It is in these layers where nonadiabatic effects are likely to be significant. It is also here that the oscillation modes are substantially influenced by convection, both via their interaction with the mean fluxes (2–4, 15, 151), or via the turbulent fluctuations (36, 139–142, 209, 210, 222, 248, 261, 262, 308). Notwithstanding these uncertainties, some progress has been made in analyzing the surface layers, most notably via the phase function $\alpha(\omega)$ appearing in Equation 3.8 (34, 71, 72, 326).

7. THE NEUTRINO PROBLEM

Perhaps the most outstanding problem related to the hydrostatic structure of the sun is raised by the neutrino deficiency. That the neutrino luminosity L_ν predicted from standard solar models is some two or three times greater than the average of the $^{37}\text{Cl}-^{37}\text{Ar}$ measurements by Davis and his collaborators (91) and also the recent Kamiokande II measurements (196) is well known (11, 13). What is not well known, however, is whether the source of the disparity is an error in solar modeling, a failure in generally accepted nuclear or particle physics, or both. Currently fashionable suggestions to modify physics generally involve neutrino transitions, either spontaneous or matter-induced, which require neutrinos to have nonzero rest mass. Some of these are directly testable by some of the new neutrino

detectors that are just coming into operation, or being planned, but others, depending on the results of the measurements, may not be. It is quite likely that an unambiguous interpretation of the results will require a knowledge of the conditions under which the neutrinos are produced.

Broadly speaking, one can classify solar-neutrino detectors into two kinds: those that are sensitive mainly to the high-energy neutrinos coming principally from ^8B decay, and those that measure the low-energy neutrinos from the p-p reaction. The signals from both the ^{37}Cl and the Kamiokande detectors are dependent predominantly on the ^8B neutrinos, which come from the energetically unimportant ppIII side chain. They are not, therefore, directly related to the energy generation rate.

As was pointed out in Section 2, theoretical standard solar models with low initial helium abundance Y_0 can reproduce the observed neutrino flux. However, such models seem unlikely, on astronomical grounds, since they require a very much lower value of the abundance ratio $Z_0 : X_0$ than is deduced from abundance analyses of stellar clusters, and because it is difficult to reconcile them cosmologically with the comparatively large primordial helium abundance believed to have been produced by the Big Bang. A direct determination of the solar Y will evidently clarify the issue.

Initial attempts to calibrate solar models seismologically suggested a value of Y_0 (about 0.30) rather higher than that which was generally accepted at the time (29, 65), which exacerbates the neutrino discrepancy. How reliably calibrations can be carried out can be judged by comparing the precision of the inversions indicated in Figure 8 with the differences between the sound speeds illustrated in Figure 1. Recent more direct determinations of Y_0 in the convection zone (see Section 6) are somewhat lower, but still seem to imply a relatively high value of L_v .

Because the frequencies of five-minute modes are relatively insensitive to conditions in the high-temperature core, diagnosis of the physical conditions in the neutrino-producing regions from currently available data is a very delicate matter. Inversions have been carried out using optimal averaging (87, 161), a regularized least-squares minimization (112, 113), and asymptotic methods (327). They have given somewhat disparate results, due partly to inadequacies that now have been recognized in the data sets (87). However, all suggest that conditions in the core are such that, if currently accepted physics is correct, the neutrino flux should probably exceed twice the observed value. This is true, in particular, of the inversion illustrated in Figure 8, provided δu and $\delta \rho$ are interpreted as static departures from the reference model of a static solar interior and the helium abundance in the core is consistent with standard stellar evolution theory.

It would be quite wrong to conclude from these results alone that

the explanation to the neutrino problem must lie in a modification to fundamental physics. All the solar calibrations, including the inversions, rely on many, if not all the simplifying assumptions listed in Section 2, and it is unlikely that all of them are correct. Whether the violation of those assumptions leads to a sufficiently severe modification to our ideas about core structure still needs to be determined, and until that is done the solar laboratory cannot be usefully employed to study nuclear and particle physics. In this regard it is interesting to note that all relevant stability calculations (29, 59, 280, 297) have found the core to be unstable to gravity modes, whose nonlinear development seems likely to be a sustained coherent oscillation (249–251). This is likely to reduce the neutrino flux somewhat (277, 278), though Dziembowski (103) has argued that the limiting amplitude is too small for the change to be significant. Issues of stability aside, an idea that has recently received some attention is that the temperature distribution in the core is flattened by a nonlocal energy transport by weakly interacting massive particles (wimps). The wimp-harboring model with an adequately low neutrino flux proffered by Gilliland et al (138a) has a high central density, which might not be inconsistent with the optimal averages illustrated in Figure 8*b*. However, it has a central sound speed some 2% lower than in the comparable standard model, which appears to be inconsistent with the inversion shown in Figure 8*a*.

A recent announcement that the Soviet-American Gallium Experiment (SAGE) (135) has obtained a preliminary null result certainly leads one to suspect that the fault in the predictions lies in particle physics. The reason is that a substantial proportion of the signal arises from the neutrinos from the p-p reaction, whose rate all theoretical models that rely on otherwise standard nuclear physics, without exception, require to be in quite close balance with the observed solar luminosity, if not precisely so. The favorite contender for the explanation is matter-induced neutrino transitions (176, 274, 299)—the MSW effect (22, 253, 332)—and physicists now are setting bounds on the arbitrary parameters in the theory of that process by reconciling the three neutrino-flux measurements (9, 130a, 217). It is evident that the outcome of the reconciliation must depend on conditions in the solar core, which thus augments the importance of the seismological diagnosis. Energy-resolving neutrino detectors planned for the future, such as the D₂O Cerenkov detector to be built in Sudbury (303), will play a crucial role in determining the details of the neutrino transitions.

8. ROTATION AND OTHER SUBSURFACE FLOWS

Rotation splits the degeneracy with respect to azimuthal order m of the oscillation eigenfrequencies. Provided the magnitude of the angular vel-

ocity Ω is much less than the oscillation frequency, which is certainly the case for all solar p modes, perturbation theory can be applied to estimate the splitting, yielding with respect to an observer in an inertial frame a contribution to the frequency shift satisfying

$$\Delta\omega \equiv (2m)^{-1}(\omega_{n,l,m} - \omega_{n,l,-m}) = I^{-1} \int [\xi \cdot \xi + m^{-1}\mathbf{k} \cdot (\xi \times \xi^*)] \Omega \rho dV \quad 8.1$$

in an obvious notation, where

$$I = \int \xi \cdot \xi \rho dV, \quad 8.2$$

the integrals being over the volume of the star. The function ξ is the oscillation eigenfunction of the corresponding nonrotating star, and ξ^* is its azimuthal conjugate, which is obtained by replacing ϕ with $\phi - \pi/2$ in the definition (Equation 3.1). It has been assumed that the sun is rotating about a unique axis defined by the unit vector \mathbf{k} , which must also be the axis of the spherical polar coordinates.

The expression on the right-hand side of Equation 8.1 arises principally from advection of the unperturbed wave form by the rotating star; it is a linear functional of Ω and affects the frequencies of otherwise similar eastward and westward propagating waves by equal amounts, but in opposite senses. If viewed from a frame rotating about \mathbf{k} with angular velocity $\Delta\omega$, the waveform resembles that found in the absence of stellar rotation. The expression can be regarded as having two parts, whose origins are most evident when Ω is uniform. The first is simply a kinematic transformation to a frame rotating with angular velocity Ω . The second, which is negative and very much smaller in magnitude, is a dynamical retardation arising from the curvature of the flow; it can be regarded as an influence of the Coriolis force when viewed from a frame rotating locally with the flow.

If Ω were a function of radius r alone, the integral constraint (Equation 8.1) would be of the form given by Equation 5.7, and the discussion in Section 5 would be directly applicable. In that case $\Delta\omega$ would be independent of m and all modes of like order and degree would precess at the same rate. In the solar photosphere, the latitudinal variation of Ω is substantially less than the mean; one might plausibly conjecture that this is also true throughout the interior (as indeed we now know it to be in the outer 50% (by radius) of the sun, as illustrated in Figure 11b). The splitting $\Delta\omega$ is then most accurately obtained from the sectoral modes, for which the magnitude of m takes its maximum value l . Indeed, it was from sectoral modes that the first inference of the angular velocity deep inside the sun was made (97). Figure 11a illustrates this result. It was obtained by a least-

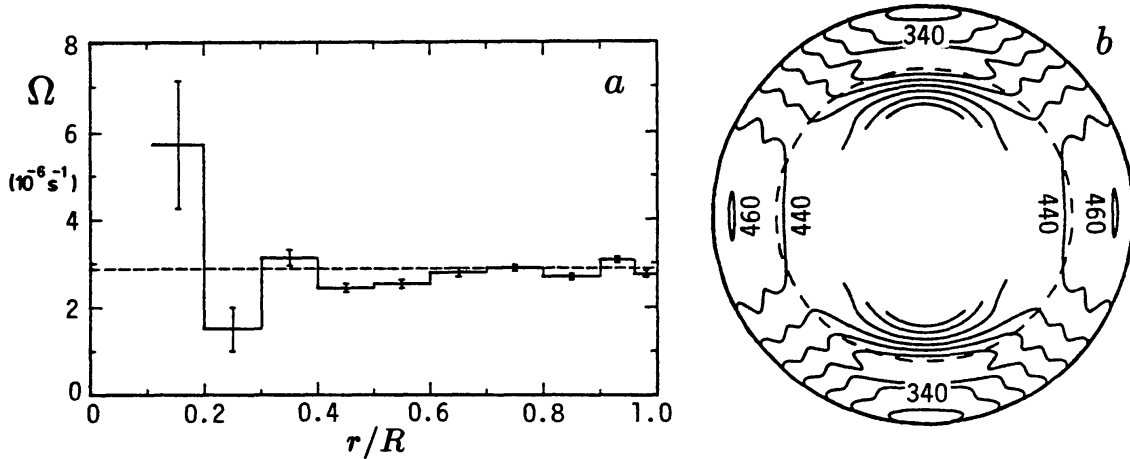


Figure 11. (a) Angular velocity in the solar interior in the vicinity of the equatorial plane [after (97)]. The error bars are formal. The dashed horizontal line indicates the photospheric angular velocity. (b) Contours of constant angular velocity in a meridional plane, inferred from (42, 73, 109, 312). The labels are values of $\Omega/2\pi$ in μHz .

squares fitting of piecewise constant functions. More detailed resolution of the rotation in the outer layers has been obtained from the splitting of modes of higher degree (174, 175, 190, 193, 213, 268, 269).

The angular velocity can also be inferred from the splitting of five-minute oscillations using asymptotic theory. The asymptotic analog of Equation 8.1 [obtained by substituting the approximation (Equation 3.5) to the eigenfunctions (Equation 3.1) into Equations 8.1 and 8.2 and ignoring the Coriolis term (or, more directly, from ray theory)] expresses the fact that $\Delta\omega$ is simply an average of Ω over that volume of the star within which the waves propagate, weighted by the relative time an acoustic wave spends in any element of volume. The formula is invertible to yield Ω as an integral of $\Delta\omega$; if Ω is independent of colatitude θ , then $\Delta\omega$ is a function of $w = \omega/L$ alone, and

$$\Omega(r) \sim W \equiv -\frac{2a}{\pi} \frac{d}{d \ln r} \int_{a_s}^a dw \int_{r_1}^R \frac{w \Delta\omega dr'}{a' r' [(w^2 - a'^2)(a^2 - w^2)]^{1/2}} \quad 8.3$$

(152), where r_1 is the radius at which $a = w$; also $a' = a(r')$, and $a_s = a(R)$ as in Equation 5.1. The outcome (151) is a smooth representation of Figure 11a.

In reality the solar rotation depends also on θ . Therefore the function illustrated in Figure 11a should be regarded as an average ($\bar{\Omega}$) of Ω over an equatorially concentrated domain within which the sectoral modes are confined. This is essentially the region $r > r_1$ outside the cones $\theta = \theta_o \equiv \sin^{-1}(m/L)$. Because, for five-minute modes, l decreases as r_1 decreases, the averages at greater depths are over domains that extend to

higher latitudes than those near the surface, which renders the interpretation of Figure 11a somewhat difficult. In particular, part of the decline of $\bar{\Omega}$ with depth comes from the decline of Ω with latitude in the outer layers of the sun. However, the observed photospheric variation of Ω with θ is insufficient to account for the entire decline; one must therefore conclude that Ω itself must decrease with depth somewhere within the domain occupied by the sectoral modes.

The θ dependence of Ω causes the frequency splitting $\Delta\omega$ to also vary with the azimuthal order m of the modes. To date the variation of $\Delta\omega$ has been made available only as an expansion in (odd-degree) Legendre functions of m/L , retaining only the first three terms. This has permitted the determination of the coefficients $\Omega_j(r)$ in the expansion in even powers of $\mu = \cos \theta$:

$$\Omega(r, \theta) = \sum_{j=1}^3 \Omega_j \mu^{2j}, \quad 8.4$$

by inverting three coupled sets of equations of the type given by Equation 5.7. It is evident from the symmetry of the integral in Equation 8.1 that odd components do not contribute to $\Delta\omega$. Several different inversion techniques have been employed (42, 73, 109, 312), the outcome of which is synthesized in Figure 11b. From this result, coupled with our knowledge of the density stratification, it is possible to compute the centrifugal distortion of the sun and hence deduce the quadrupole moment J_2 of the exterior gravitational potential (166); indeed, this is the most accurate method available for measuring J_2 . The result is $J_2 \simeq 1.5 \times 10^{-7}$; there is some uncertainty arising from our not yet having obtained Ω at high latitudes for $r \lesssim 0.5R$, but in this region the contribution to the centrifugal distortion is relatively small. With this value we may safely conclude that the radar ranging measurements of the orbit of Mercury (292, 330) confirm the predictions of General Relativity.

Recently Lavelle & Ritzwoller (226) have shown that by expressing Ω in terms of an expansion of toroidal vectors a representation can be found in which the integral constraints decouple; this involves expanding the frequency splitting in different basis functions. There is thus an apparent simplification of the analysis, but whether the procedure is preferable surely rests on the error propagation, which has not yet been investigated.

Alternatively one can carry out a direct two-dimensional inversion of the constraints (Equation 8.1). This might be advantageous particularly when the resolution of the m dependence is high, and many terms in the expansion of $\Delta\omega$ would be necessary to represent the details. According to asymptotic theory, $\Delta\omega$ is now a function of w and

$M \equiv \cos \theta_\circ = (1 - m^2/L^2)^{1/2}$. Hence the function W defined by Equation 8.3 depends on r and M ; and $\Omega(r, \mu)$ can be obtained directly from the integral (160, 216)

$$\Omega \sim \frac{\partial}{\partial \mu} \int_0^\mu \frac{W(r, M) M dM}{\sqrt{\mu^2 - M^2}}. \quad 8.5$$

Alternatively one can perform a direct numerical inversion, either by constructing two-dimensional optimal localized averages (e.g. 285) or by minimizing a two-dimensional generalization of a measure such as $E + \lambda D$ discussed in Section 5. Sekii (287, 288) has used the latter method.

When l is large the distortion of the eigenfunctions due to the advection is not insignificant (333). One way to attempt to account for this when analyzing observations is to project the signal onto appropriately distorted eigenfunctions. This would be practical only if one had some idea of the distortion, which might be determined by iteration. Alternatively one can regard the distorted mode as a superposition of local plane waves, each of which is advected locally by the horizontal component of the mean flow \bar{U} beneath (163). Then one can investigate the entire flow, including both rotation and, perhaps, giant convective cells, in a straightforward manner. If one plots the local dispersion relation at constant frequency ω in the $k_x - k_y$ plane, where k_x and k_y are orthogonal components of the horizontal wavenumber in the photosphere, the result is a sequence of rings, each corresponding to a single value of the order n ; they are approximately circular and displaced from the origin by an amount that depends on \bar{U} (160, 183, 184), as shown in Figure 12. Hill (183–186) has inverted these displacements to obtain not only the horizontal variation but also the depth dependence of the flow.

9. MODE EXCITATION AND DECAY

It is most likely that p modes are intrinsically stable, and are excited randomly by the turbulence in the convection zone. This is, perhaps, the earliest proposal to have been investigated in some detail, though in the years immediately following the discovery of the five-minute oscillations it was believed to be the resonant response of just the atmosphere above the convection zone that picked out characteristic frequencies. A mode can be regarded as a damped simple harmonic oscillator, satisfying the model equation

$$I \left(\frac{d^2 q}{dt^2} + 2\gamma \frac{dq}{dt} + \omega_0^2 q \right) = F(t), \quad 9.1$$

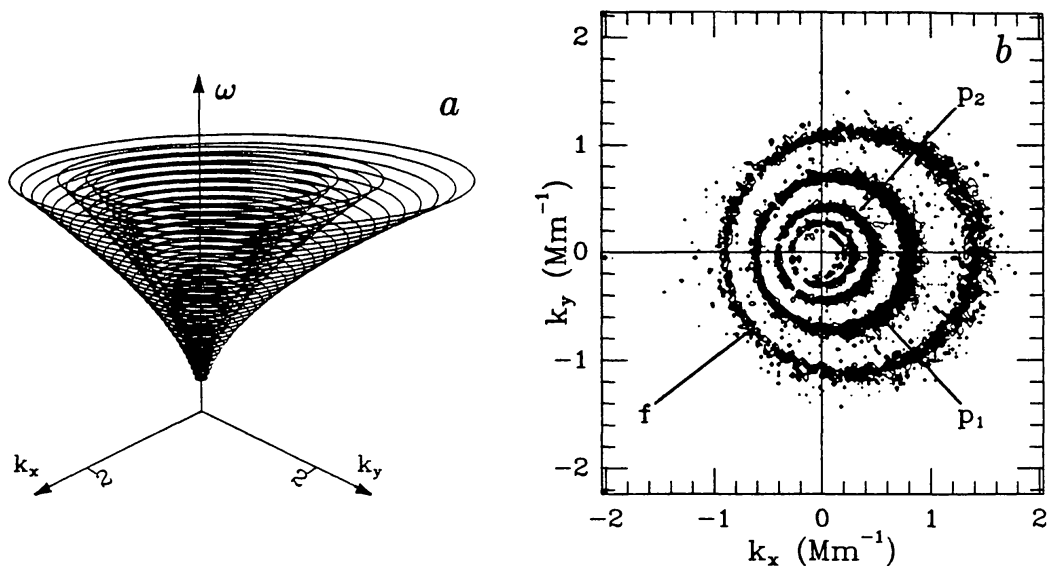


Figure 12 (a) Schematic representations of the mode frequency ω as a function of horizontal wavenumber (k_x, k_y) in the presence of a horizontal flow in the positive x direction. (b) Power spectrum of observations at constant cyclic frequency $\nu = 2862 \mu\text{Hz}$ in the vicinity of the solar equator, where k_x and k_y are the eastward and northward components of the horizontal wavenumber, respectively measured in Mm^{-1} . To achieve more uniform visibility, the power has been enhanced by a factor k^2 [from (183)].

where q is a measure of the surface displacement, I is the inertia of the mode, defined such that $\frac{1}{2}I(\dot{q}^2 + \omega_0^2 q^2)$ is the total energy E associated with the oscillation, and F is a random forcing function. This problem was considered by Batchelor (18), who showed that the power spectrum P_q of q satisfies

$$P_q(\omega) \simeq \frac{1}{4\omega_0^2} \frac{P_F(\omega)}{(\omega - \omega_0)^2 + \gamma^2} \quad 9.2$$

for frequencies near ω_0 , where P_F is the power spectrum of F . For $\gamma \ll \omega_0$, which is the case for modes with frequencies well below the acoustic cutoff in the atmosphere, the spectrum is strongly peaked near $\omega = \omega_0$ with a Lorentz profile whose full width at half maximum is $\Gamma = 2\gamma$. Furthermore, the energy E satisfies

$$\frac{dE}{dt} + \Gamma E = G, \quad 9.3$$

where $G = \langle \dot{q}F \rangle$ is the mean rate of working of the force F on the mode, the angular brackets denoting an appropriate average over a period of oscillation. Thus the equilibrium energy is given by

$$E = \frac{G}{\Gamma}. \quad 9.4$$

Central to the theory is the difficult task of evaluating the power input G . The quantity $\langle \dot{q}F \rangle$ is actually not only an average over time but is also an integral over the volume occupied by the turbulence that is exciting the oscillations. Lighthill (243, 244) in his pioneering work showed how G could be estimated for free turbulence in an unstratified fluid: Provided the Mach number M of the characteristic velocity u of an eddy is much less than unity, the eddy radiates as a quadrupole source at a rate

$$g \propto \rho u^3 l^2 M^{2k+1} \quad 9.5$$

with $k = 2$, where ρ is the density and l is the characteristic length scale of the eddy. Moreover, the acoustic emission has a characteristic frequency ω commensurate with the rate of change of the energy in the eddy:

$$\omega \simeq \omega_e \equiv u/l. \quad 9.6$$

In reality, there is a distribution of ω_e , and if the eddies are uncorrelated, the total power G in a given frequency interval can thus be obtained by integrating g over all eddies with values of ω_e within that interval.

Quadrupole acoustical emission by free turbulence in an unstratified medium is a consequence of mass and momentum conservation: Monopole emission ($k = 0$) requires substantial dilatation of the turbulent flow, and dipole emission ($k = 1$) requires the action of external forces. Compressible turbulent convection, however, is stratified under gravity, and is driven by buoyancy forces. Therefore both monopole and dipole emission is likely to occur, as Unno (321) has pointed out. For turbulence with very low Mach number, the monopole emission must dominate. But at values as great as 0.2, which might be encountered near the top of the solar convection zone, the dominant source could be different. Indeed, Stein (306) has estimated that the emission by turbulence with $M = 0.1$ in an isothermal atmosphere is dominated by quadrupole emission.

The evaluation of Γ is an even more difficult task. Christensen-Dalsgaard & Frandsen (62) have demonstrated that energy exchange with radiation can be treated adequately by the Eddington approximation, and it would be relatively straightforward to estimate the energy leakage from the star if the structure of the upper atmosphere were steady and smooth. However, in reality there are magnetic fields and fluctuating horizontal structural inhomogeneities which principally absorb and scatter global modes into smaller-scale waves, thereby contributing to their decay. Turbulent fluctuations in the convection zone do likewise. The study of these processes, both observationally (30, 31, 172, 173, 175) and theoretically

(24–28, 198, 246, 275, 276, 305), is in its infancy, but it is likely to develop substantially in the near future. Another serious problem is to determine the energy exchange between the convection and the oscillation resulting from the modulation of the Reynolds stresses and the convective heat flux by the oscillations. Prescriptions for statistically steady turbulent convection are not reliable; prescriptions for time-dependent convection are even less so.

The first attempt to combine the elements of the theory to estimate both Γ and G , and hence estimate E from Equation 9.4, was made by Goldreich & Keeley (139, 140). The damping rate Γ was obtained from a linear stability computation, treating radiation in the Eddington approximation, introducing a simple phase lag to the convective enthalpy flux computed from mixing-length theory, and modeling the Reynolds stress with a scalar viscosity produced by eddies with $\omega_e > \omega$ and chosen to ensure that the modes are intrinsically stable. The power G was obtained by estimating $\langle \dot{q}F \rangle$ from the oscillation eigenfunctions using order-of-magnitude estimates for the turbulent fluctuations. Here quadrupole emission was assumed to dominate. Thus it was found that the turbulence appears to drive the oscillations only to an amplitude substantially smaller than observed. In particular, at frequencies near 3 mHz, the amplitudes were about 4% of those currently reported.

It should be emphasized that the amplitude estimates are extremely rough. First, the value of G is sensitive to the power spectrum assumed for the turbulence (306). Second, the uncertainties in the mixing-length estimates of the fluctuating stresses could easily be wrong by a factor of four or more, even after constraining the formalism by the solar calibration discussed in Section 2, which could lead to a modification of the value of G by a factor 10^2 or so (147). A third point to mention, which is related to and perhaps contained in the other two, is that because the energy of an eddy in a stellar convection zone is a rapidly varying function of its characteristic time scale, the insertion of a factor of order unity in the resonance condition (Equation 9.6) makes a substantial difference to the magnitude of G . Therefore the discrepancy between Goldreich & Keeley's estimates and the observations does not necessarily vitiate the stochastic excitation hypothesis. Indeed, scaling the turbulent velocities by a factor of order unity brings the estimates into approximate agreement with observation (15, 63, 149), particularly if observed line widths are used for Γ .

Recently, there have been renewed efforts to understand the excitation. Goldreich & Kumar (141, 142, 222, 223) and Osaki (257) have rediscussed the random excitation process. By approximating the convection zone by an adiabatically stratified polytrope, Goldreich & Kumar (142) found that the eigenfunction is almost orthogonal to the sum of the monopole and

dipole forcing terms, yielding only a quadrupolar remnant. However, the major contribution to the high-frequency p modes comes from the upper convective boundary layer, where the stratification is not adiabatic and cancellation is presumably not complete. Osaki (257) has argued that even so, the dominant emission is still quadrupolar. The reason is that convective motion is not purely random, for downflow is usually immediately surrounded by upflow, and consequently adjacent sources of dipole radiation are oppositely oriented within an acoustically compact region. There would similarly be some destructive interference reducing the strength of the monopole radiation.

Numerical three-dimensional simulations of the upper layers of the solar convection zone carried out by Nordlund & Stein (307, 308) also exhibit acoustic-mode excitation, as do simulations of compressible convection invoking simpler physics (45, 46, 209, 210, 247, 248, 316). Such computations promise to provide a valuable testing ground for future theories.

From measurements of the surface amplitudes q , E can be computed from the eigenfunctions; and if an equation like 9.1 is valid, Γ can be measured from the line widths of the power spectrum. Hence, by using Equation 9.4, G becomes a measured quantity. Libbrecht et al (237, 238) and Elsworth et al (120) measured the frequency dependence of Γ , whose basic features were found to be in tolerable agreement with existing theoretical computations that had taken into account (albeit in an approximate way) the modulation of the turbulent momentum and energy fluxes by the oscillations (67). More recent calculations (16) have been tuned to agree with the observations more closely. Libbrecht (234) has also shown that for $v = \omega/2\pi \lesssim 4$ mHz, $G \propto \omega^8$, and that for $v \gtrsim 5$ mHz, $G \propto \omega^{-5.5}$.

Some progress has been made towards finding a natural explanation to these simple results. Using the frequency responses calculated by Goldreich & Kumar (141), Osaki (257) estimated that $G \propto \omega^{-5.5}$ at frequencies above the characteristic value of ω_e in the region where the turbulent energy density is greatest; and by representing the convection zone as a polytrope of index μ , he estimated that $G \propto \omega^{2\mu}$ for $\omega \lesssim \omega_e$. Goldreich & Kumar (142), using a somewhat more sophisticated argument, found $G \propto \omega^{(2\mu^2 + 7\mu + 3)/(\mu + 3)}$ in the low-frequency limit. Both low-frequency estimates agree with Libbrecht's finding (illustrated in Figure 13) provided $\mu = 4$, a value which is not atypical of the convective boundary layer.

In concluding, we mention the possibility of acoustic modes being linearly unstable, as is the case in classical intrinsically variable stars (1–3, 317). The most obvious problem that is immediately encountered is to explain why the amplitudes of the oscillations are so low. Kumar & Goldreich (223) have examined theoretically the nonlinear interactions between modes in a model solar envelope, and conclude that the energy

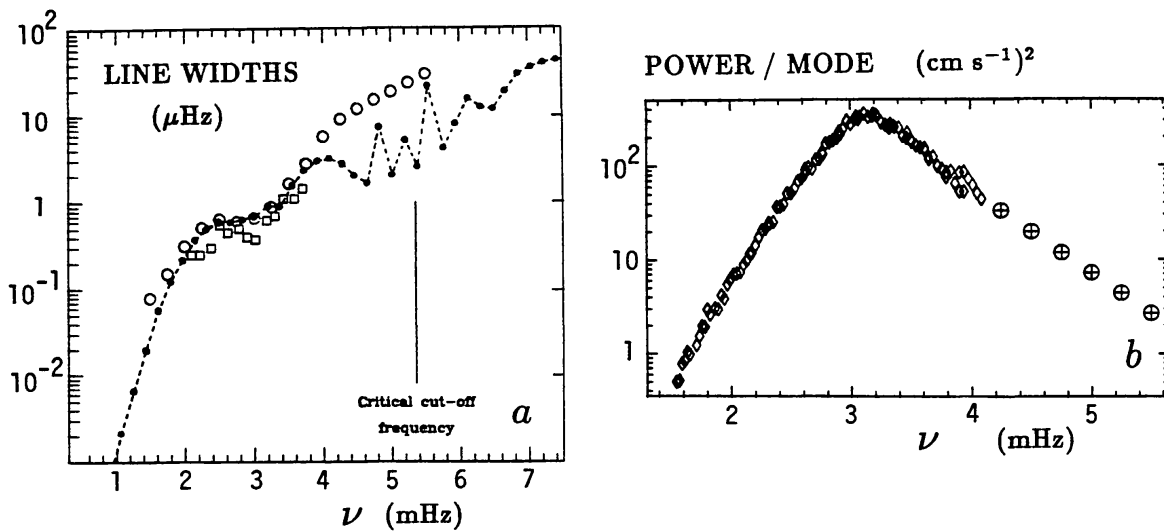


Figure 13 (a) Linewidths of low-degree p modes measured by Libbrecht (233, 234) (open circles) and Elsworth et al (120) (squares). The filled circles joined by dashed lines are theoretical estimates of damping rates of radial modes (16). The acoustical cutoff frequency in the atmosphere is indicated. (b) Power per mode, measured by Libbrecht (234).

transferred into damped waves is insufficient to limit the amplitudes of the unstable modes to their observed values. Turbulent excitation of stable oscillations is therefore more likely, at least for the 5-minute p modes. If that is indeed the case, then, because the energy input to the waves varies as such a high power of the turbulent velocity, the acoustic sources are likely to be compact and well dispersed, and hence susceptible to detection by observation (41).

10. SOLAR-CYCLE VARIATIONS

Asphericity Variation

The frequency perturbation by advection due to rotation that is discussed in the previous section is the only contribution to degeneracy splitting that is an odd function of m . All other symmetry-breaking agents cannot distinguish between east and west, and therefore their contribution to the frequency splitting cannot depend on the sign of m . Their influence on the oscillation frequencies can be divided into two parts: their direct effect on the dynamics of the oscillations and their indirect effect arising from the distortion they inflict upon the basic state of the sun.

The large-scale deviation of the solar structure from spherical symmetry is small in magnitude—of order 10^{-4} . Therefore, as with rotation, perturbation theory can be used to estimate the splitting. The outcome is a set of integral relations for the even component of the splitting which,

broadly speaking, are similar to Equation 8.1. The integrals are averages of the splitting agent, which could be centrifugal force, Lorentz force, or an asphericity in the basic state of the sun, weighted by a kernel which depends on the unperturbed eigenfunctions of oscillation (106, 108, 146, 160, 166, 272). Therefore the methods available for inverting the relations (8.1) can also be applied to the even component of the splitting.

It is not an easy matter to unravel the influences of different symmetry-breaking agents. Indeed, it is probably not even possible in principle, particularly if data from only five-minute modes are available. One can obtain the angular velocity Ω from the odd component of the splitting, and from it calculate the rotational contribution to the even component that arises from the centrifugal force and corrections to the advection term arising from the rotational distortion of the eigenfunctions (109, 166). The remainder is due to everything else, and may therefore eventually play the role of calibrating theories rather than making unambiguous inferences.

To date, the even component of the degeneracy splitting of intermediate and high-degree modes has been approximated by truncated expansions of the kind

$$\frac{1}{2}(\omega_{n,l,m} + \omega_{n,l,-m}) - \omega_{n,l,0} \simeq 2\pi \sum_{k=1}^2 \alpha_{2k} P_{2k}\left(\frac{m}{L}\right), \quad 10.1$$

the coefficients α_{2k} being presented often as averages over n and over specified ranges of l . The first observations, by Duvall et al (101), yielded coefficients α_{2k} that were substantially larger than would be produced by the centrifugal force estimated for Figure 11, and, moreover, of the opposite sign (165): In other words, the sun was acoustically prolate.

What is the nature of the asphericity? Under the assumption that it is confined to the convection zone, supported hydrostatically by a spherically symmetrical radiative interior, the latitudinal variation in the wave propagation speed appears to be more likely the direct effect of magnetic fields in the surface layers, possibly in fibril form, rather than due to a thermal variation of the sound speed (165). The reason is that if the asphericity were thermally induced, the constraints imposed by almost hydrostatic balance and the observed frequency splitting would require the photospheric temperature in the equatorial regions to be much too low. Nevertheless it is interesting, though perhaps fortuitously coincidental, that observed latitudinal variations of surface brightness temperature (221)—if they are interpreted as a thermodynamical temperature variation and if in addition the relative temperature variation is simply assumed to persist to a depth of 5% or more of the solar radius—could be made to reproduce the splitting data (219, 220). However, the precise frequency deter-

minations reported recently by Libbrecht & Woodard (239, 240), some of which are illustrated in Figure 5, are consistent with almost all the asphericity being concentrated in the very outer layers of the sun (17, 143, 239, 240), extending perhaps no more deeply than the superadiabatic convective boundary layer: less than 2% of the solar radius. Nevertheless, Goode & Kuhn (146) argued that this might result from thermal shadowing (260) behind a magnetic field situated near the base of the convection zone.

The observations of Libbrecht & Woodard (239, 240) show a systematic difference between the asphericity in 1986, near sunspot minimum, and 1988, roughly half-way up the rising branch of the cycle. This difference is impressively similar to the brightness-temperature variation reported by Kuhn and associates (221), and is suggestive of the brightness temperature being modulated by small-scale magnetic activity which also modulates the oscillation frequencies, either beneath the photosphere (165, 338, 339) or in the chromosphere (47, 121, 272). Of course, measurements at only two epochs do not demonstrate a solar-cycle variation. An association with the solar cycle has been claimed from correlation analyses of whole-disk low-degree frequency data over the last 11 years (118, 136, 259, 336), the most extensive data set being that of Elsworth et al (118). Degeneracy splitting has not been resolved, but the shifts in the line-centers are consistent with what one would expect from the variations inferred by Libbrecht & Woodard from modes of intermediate and high degree. Frequency shifts over an interval of a few months during 1989 obtained from whole-disk intensity observations from the spacecraft *Phobos* (129) are also consistent with the earlier data.

Although most of the degeneracy splitting is produced by an asphericity in the surface layers of the sun, there appears to be a residual component whose origin is more deeply seated. Inversions of the data have indicated that the cause of the residual splitting is located near the base of the convection zone, and has been interpreted as the direct influence of an equatorially concentrated megagauss azimuthal magnetic field (106–108). Dziembowski & Goode (108) found no evidence of the field changing with time.

Whether there is a cyclic variation in the solar structure well beneath the convection zone remains an open question. Correlations of neutrino-flux variations with sunspot number have been claimed (10, 12, 23, 90, 218), though their significance is in some doubt (122). The most popular suggestion for explaining the neutrino variations is a modulation of a constant source by neutrino helicity flipping caused by the solar magnetic field in the outer layers of the sun. The most naive thought, however, would be that the source itself is varying, but unfortunately current seismic data are inadequate to resolve that issue.

Correlation with Magnetic Activity and Brightness Temperature

The splitting coefficients α_{2k} vary with time, and are correlated with the solar cycle, with larger splitting occurring at sunspot maximum (159, 219). Recent analysis by Libbrecht & Woodard (239, 240) of the frequency dependence of temporal variation of both the splitting and the absolute frequencies shows them to be inversely proportional to the modal inertia I . This implies that the variation in the solar structure occurs predominantly in the surface layers, where I is normalized.

The latitudinal variation deduced from the splitting coefficients is in excellent agreement with the distribution of brightness-temperature variations (239, 240) measured by Kuhn et al (221). Nevertheless, one cannot conclude from this agreement that the perturbations to the frequencies arise from corresponding variations in the gas temperature. Indeed, hydrostatically consistent thermal perturbations seem unlikely to be able to account for both the frequency variations and the solar irradiance variations (331) measured from ACRIM on the *Solar Maximum Mission* (17, 143, 165). Magnetic perturbations may be responsible, either directly or indirectly through their influence on convective velocities (cf 36), both for the frequency changes and for the variations in brightness temperature.

Angular Velocity Variation

Goode & Dziembowski (144, 145) have analyzed the odd components of the frequency splitting obtained by Libbrecht & Woodard (239) in 1986 and 1988. They found some evidence of an angular velocity change about halfway out from the center of the sun, whereas at the base of the convection zone the variation was absent. This tantalizing result, which is consistent with an earlier analysis by Goode et al (145), seems to imply that the radiative interior takes part in the solar cycle, and leaves one wondering whether the cycle is really controlled by a dynamo, as is commonly believed, or by large-scale torsional oscillations of the entire sun. It must be appreciated, however, that this result is barely significant, and is challenged by more recent inversions by Schou (284).

11. ASTEROSEISMOLOGY

It is natural to expect that solar-type stars should oscillate with amplitudes similar to those of the sun. Christensen-Dalsgaard & Frandsen (63) have estimated the stochastic excitation in late-type zero-age main-sequence stars, and predicted oscillation amplitudes in stars with masses near $1.5 M_\odot$.

to be more than ten times greater than those of the sun. Instrumentation is now approaching a state that should make observation of such oscillations possible (40, 123, 177).

In the early stages of the development of asteroseismology we can expect to measure only the lowest-degree modes in distant stars, as have been detected in whole-disk measurements of the sun. One might anticipate that progress will be similar to the solar case, and that initially just the four quantities ω_0 , μ , A , and B defined by Equations 3.10–3.13 will be available from superposed power spectra. These will add immensely to the classical astronomical information, and can in principle be used to calibrate theoretical models and hence to estimate important properties of the star.

The parameter ω_0 measures the acoustical radius, which is a gross property of the entire star. It scales as $M^{1/2}R^{-3/2}$ under homology transformation, which is certainly a good first guide for stars that do not differ greatly from the sun. The parameter A measures the average sound-speed gradient, weighted predominantly in the core where r^{-1} is large. Thus it is sensitive to the molecular-weight variation produced by the nuclear reactions, and is therefore an indicator of age. Finally, μ and B measure conditions mainly in the outer layers of the stellar envelope, and in principle should be usable to determine a relation between surface gravity and effective temperature.

The potential of ω_0 and A , as measured by mean values of $\omega_{n,l} - \omega_{n-1,l}$ and $\omega_{n,l} - \omega_{n-1,l+2}$ respectively, was emphasized by Christensen-Dalsgaard (50–52) with a diagram similar to Figure 14. This shows the theoretical evolutionary tracks of a series of main-sequence stars of uniform initial chemical composition. If the composition were known, one would evidently pinpoint the mass and age of the star from a knowledge of its position on that diagram. However, chemical composition is not known: Although the ratio of the total heavy-element abundance Z to the hydrogen abundance X can be determined spectroscopically, the absolute abundances can not, and one must appeal to other astronomical measurements to calibrate the models. A sensitivity analysis (158) based on the properties of theoretical solar models discussed by Ulrich (319, 320) indicated that the major source of uncertainty generally arises from errors in Z/X . With the estimated errors of 10%, which appear to be achievable for stars in clusters (263, 300, 304), this leads to errors of perhaps 20% in the estimates of both mass and age. It should be possible to substantially reduce the errors for binary stars that are sufficiently separated for mass transfer not to have occurred, particularly if the masses have been determined (40).

An unambiguous detection of p -mode oscillations of sun-like stars has not yet been made. Evidence of approximately uniformly distributed peaks in power spectra, as indicated by the leading term of Equation 3.10, has

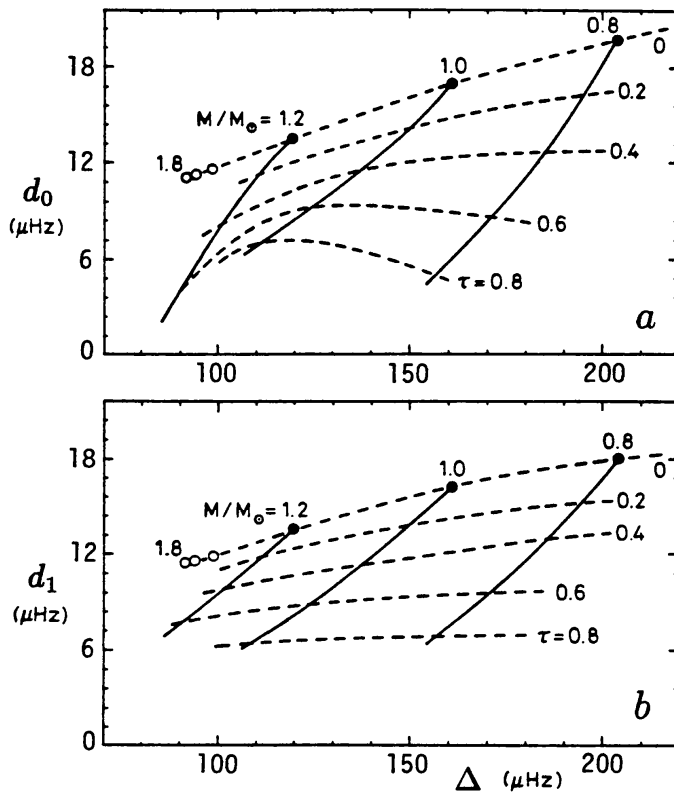


Figure 14 Dependence of d_0 and d_1 on Δ , where $2\pi d_l$ is an average over n of $\omega_{n,l} - \omega_{n-1,l+2}$ of 5-minute modes and Δ is an average over n and l of $\omega_{n,l} - \omega_{n-1,l}$ for models of late-type main-sequence stars. The *continuous lines* are at fixed mass M , and therefore represent the evolution of stars; the *dashed lines* are contours of constant evolution age $\tau = t/t_n$, where t is time measured from arrival on the main sequence and t_n is the age at central hydrogen exhaustion [from (158) based on computations by Ulrich (319, 320)].

been found as a peak in a power spectrum of the power spectrum of oscillations of a few stars (19, 20, 42a, 77, 125, 126, 138, 204, 205, 255, 301), and thus provides a first estimate of ω_0 . There is evidence for several discrete frequencies in the intrinsic variation of Arcturus (19, 205), but unfortunately it has not yet been possible to carry out observations that are sufficiently long with an adequate duty cycle to isolate unambiguously any but perhaps one of the modes. Greater success has been achieved with the higher-amplitude pulsating Ap stars by Kurtz and associates (224), who have successfully isolated individual modes of oscillation; however, the pulsations of these stars evidently depend strongly on a large-scale asphericity associated with a strong magnetic field, the discussion of which is outside the scope of this review.

Seismological diagnosis is likely to be extended to other stars too, such as white dwarfs, some of which appear to pulsate in many modes

simultaneously. The methods by which the data will be analyzed and the prospects for success have been discussed in several recent reviews (50, 83, 85, 93, 104, 105, 211).

12. CONCLUDING REMARKS

We have come a long way since 1984 when the last article on solar oscillations appeared in *Annual Reviews*. At that time seismologically useful data were just becoming available, and serious inversion studies had hardly begun. Since then there has been a substantial increase in both the quality and quantity of data that have been acquired; and from them it has already been possible to make useful inferences about conditions deep inside the sun.

The most basic inference concerns the hydrostatic stratification, most notably its spherically symmetric component. This is illustrated in Figure 8, in which localized averages of the logarithmic differences $\delta u/u$ and $\delta \rho/\rho$ between the sun and a standard solar model are plotted. Because the perfect gas law is not far from the true equation of state, the quantity $u = p/\rho$ is approximately proportional to T/μ , where T is temperature and μ is the mean molecular mass. Thus the region $0.3 \lesssim r/R \lesssim 0.7$ in which $\delta u > 0$, and which appears to be where inversions are the most robust, probably signifies that the temperature in the sun is higher than in the model. It is unlikely to have resulted from a local deficiency of helium; though some degree of gravitational settling of helium has no doubt taken place, present computations suggest that it is insufficient to explain the data. Indeed, with the first sound-speed inversion in the radiative interior it was suggested that the temperature in the above region is the consequence of having underestimated opacities where the temperatures are a few million degrees, causing the sun to be hotter than the model in and immediately below that region. Five years later, more highly resolved opacity computations undertaken at Livermore have confirmed this prediction.

Other properties of inversions are worthy of mention. In particular, the base of the convection zone can be detected as a discontinuity in the second derivative of u , and has now been located apparently to within 0.3% of the solar radius. In addition, it has been possible to measure the influence of ionization on acoustic propagation, and thereby with the help of the equation of state attempt to infer the helium abundance in the convection zone. It now appears that the weakest link in the current chain of inferences is not seismological, but is an inadequacy in our knowledge of the equation of state. Thus in future the reasoning must become more intricate as the solar convection zone becomes a laboratory for developing the physics of dense plasmas.

Hints about the structure of the solar core are quite exciting. Figure 8 suggests a quite sharp deviation, particularly in u , between the sun and the reference theoretical model at $r \simeq 0.2R$, inside of which most of the nuclear reactions take place. Great care must be taken in trying to interpret this property. There is, of course, a strong temptation to do so solely in terms of standard theory, and arguments that rest on standard theory should certainly be considered very seriously. But one should not lose sight of the fact that many of the assumptions listed in Section 2 have not been well justified. Moreover, because acoustic modes spend so little time in the high-temperature core, the contribution made by the core to their frequencies is relatively small, as is evident in Figure 4, and therefore the inferences made for $r \lesssim 0.2R$ are insecure. What is sorely needed is the identification and measurement of just a few g modes, whose kernels are concentrated in the central regions of the sun. It is a responsibility of helioseismologists to devote a substantial effort in this direction, in order to provide more reliable information for particle physicists about the conditions in which the nuclear reactions are taking place. It is to be hoped that the new generation of seismological observations, both from ground-based networks and from space, will provide that information in time for the next generation of neutrino detectors.

Deviations from sphericity have also been investigated seismologically. The most detailed information has come from rotational splitting, which is produced essentially by advection of the acoustic waves. It has been possible to obtain an estimate of the solar angular velocity Ω in the vicinity of the equatorial plane down to about the edge of the energy-generating core, and to obtain an indication of the latitudinal dependence in the outer 50% (by radius) of the star. This is illustrated in Figure 11. Fortunately, the determination encompasses the region where the influence of the centrifugal force on the shape of the sun is greatest, and thus with only a little significant extrapolation we are able to calculate the asphericity of the matter distribution, and hence determine the quadrupole moment J_2 of the exterior gravitational potential. At present this is the most reliable method for determining J_2 , and is likely to remain so for a long time. Together with laser ranging data, it provides a test of theories of gravitation via orbital precession, the results of which are quite consistent with General Relativity.

There are other interesting properties of the angular velocity illustrated in Figure 11. Perhaps most notable is the near constancy of Ω (except possibly in the core, but the pertinent data are not reliable), and, more interestingly, the hint of a decline of Ω with depth at low latitudes through much of the radiative interior. Before this result had been obtained, theorists predicted that as a result of the retarding torque applied by the

solar wind the radiative interior would probably not have spun down in step, and that therefore Ω should rise substantially with depth. Only those who believed that a large-scale magnetic field of at least $3 \mu\text{G}$ pervades the interior, which is hardly implausible, thought that Ω should be nearly constant. But nobody seems to have suggested that Ω actually declines with depth.

Of course the angular velocity may not be steady, and a component of the variation evident in Figure 11 might be a manifestation of a temporal oscillation associated, perhaps, with the solar cycle. The shear layer at the base of the convection zone, which is too thin presently to be resolved, is no doubt also dynamically important, and must wind any poloidal magnetic field present in that region into an azimuthal coil. This process is also likely to be intimately connected with the solar cycle.

Other properties of the frequency spectrum are now seen to be varying with the solar cycle. There are both gross frequency shifts and variations in the splitting, indicating that both spherical and aspherical structural changes occur. The frequency dependence of these variations indicates that most of the structural change in the sun takes place in the vicinity of the photosphere, where most acoustic modes are evanescent. These are probably connected with a modulation of the geometry and intensity of the surface magnetic field, which is no doubt controlled by the convection. It will probably be necessary to await the next generation of observations with GONG and SOI before the convective flow can be investigated with adequate reliability to shed light on the dominant dynamical processes. There is also some evidence for a temporally varying component of the frequency splitting whose origin lies deeper within the sun. Once again, it is hoped that the next generation of data will be sufficiently accurate and extensive to reveal whether that is actually so.

Finally, we are probably now at the dawning of asteroseismology. There are observational hints for a spectrum of oscillations in a few solar-type stars, and there are other classes of stars, such as Ap stars and white dwarfs, where several, if not many, frequencies are present. Imminent progress, both observational and theoretical, will thereby open up a new and powerful astronomical technique for investigating the interiors of stars.

ACKNOWLEDGMENTS

This work was partly supported by the National Aeronautics and Space Administration through grants NSG-7511, NAGW-91, and contract NAS 5-30386, and by the U.K. Science and Engineering Research Council. We have appreciated the thoughtful advice and detailed help provided by the

many participants in the six-month research program in helioseismology recently conducted at the Institute for Theoretical Physics (ITP), University of California at Santa Barbara. The spirited discussion and debate at ITP on scientific issues central to helioseismology helped to clarify our perspective on many matters. The ITP program was partly supported by the National Science Foundation through grant PHY89-04035 and partly by NASA funds, and especially by funded research leaves of absence from various home institutions, including those of the authors. We are grateful to A. G. Kosovichev for his help in producing the diagrams.

Literature Cited¹

1. Ando, H., Osaki, Y. 1976. *Publ. Astron. Soc. Jpn.* 27: 581–603
2. Antia, H. M., Chitre, S. M., Gough, D. O. 1988. In AARHUS, pp. 371–74
3. Antia, H. M., Chitre, S. M., Narashima, D. 1982. *Sol. Phys.* 77: 303–27
4. Antia, H. M., Chitre, S. M., Pandey, S. K. 1981. *Sol. Phys.* 70: 67–91
5. Backus, G., Gilbert, F. 1967. *Geophys. J. R. Astron. Soc.* 13: 247–76
6. Backus, G., Gilbert, F. 1968. *Geophys. J. R. Astron. Soc.* 16: 169–205
7. Backus, G., Gilbert, F. 1970. *Philos. Trans. R. Soc. London Ser. A* 266: 123–92
8. Bahcall, J. N. 1989. *Neutrino Astro-*
physics. Cambridge: Cambridge Univ. Press
9. Bahcall, J. N., Bethe, H. 1990. *Phys. Rev. Lett.* 65: 2233–35
10. Bahcall, J. N., Field, G. B., Press, W. H. 1987. *Ap. J.* 320: L69–73
11. Bahcall, J. N., Huebner, W. F., Lubow, S. H., Parker, P. D., Ulrich, R. K. 1982. *Rev. Mod. Phys.* 54: 767–99
12. Bahcall, J. N., Press, W. H. 1991. *Ap. J.* 370: 730–42
13. Bahcall, J. N., Ulrich, R. K. 1988. *Rev. Mod. Phys.* 60: 297–372
14. Deleted in proof
15. Balmforth, N. J., Gough, D. O. 1990. *Sol. Phys.* 128: 161–93
16. Balmforth, N. J., Gough, D. O. 1990. *Ap. J.* 362: 256–66
17. Balmforth, N. J., Gough, D. O., Merryfield, W. J. 1991. *MNRAS.* Submitted
18. Batchelor, G. K. 1956. *The Theory of Homogeneous Turbulence.* Cambridge: Cambridge Univ. Press
19. Belmonte, J. A., Jones, A. R., Pallé, P. L., Roca Cortés, T. 1990. *Ap. J.* 358: 595–609
20. Belmonte, J. A., Peréz Hernández, F., Roca Cortés, T. 1990. In HAKONE, pp. 417–24
21. Berthomieu, G., Cooper, A. J., Gough, D. O., Osaki, Y., Provost, J., Rocca, A. 1980. In *Nonlinear and Nonradial Stellar Pulsation*, ed. H. A. Hill, W. A. Dziembowski, pp. 306–12. Heidelberg: Springer
22. Bethe, H. 1986. *Phys. Rev. Lett.* 56: 1305–8
23. Bieber, J. W., Seckel, D., Stanev, T., Steigman, G. 1990. *Nature* 348: 407–11
24. Bogdan, T. J. 1989. *Ap. J.* 339: 1132–49
25. Bogdan, T. J. 1989. *Ap. J.* 345: 1042–49
26. Bogdan, T. J., Cattaneo, F. 1989. *Ap. J.* 342: 545–57

27. Bogdan, T. J., Zweibel, E. G. 1985. *Ap. J.* 298: 867–75
28. Bogdan, T. J., Zweibel, E. G. 1987. *Ap. J.* 312: 444–56
29. Boury, A., Gabriel, M., Noels, A., Scufflaire, R., Ledoux, P. 1975. *Astron. Astrophys.* 41: 279–85
30. Braun, D. C., Duvall, T. L. Jr., Jefferies, S. M. 1990. In HAKONE, pp. 181–87
31. Braun, D. C., Duvall, T. L. Jr., LaBonte, B. J. 1988. *Ap. J.* 335: 1015–25
32. Brodsky, M. A., Vorontsov, S. V. 1987. *Sov. Astron. Lett.* 13: 179–81
33. Brodsky, M. A., Vorontsov, S. V. 1988. In AARHUS, pp. 137–40
34. Brodsky, M. A., Vorontsov, S. V. 1988. In TENERIFE, pp. 487–91
35. Brookes, J. R., Isaak, G. R., van der Raay, H. B. 1976. *Nature* 259: 92–95
36. Brown, T. M. 1984. *Science* 226: 687–89
37. Brown, T. M. 1984. In SNOWMASS, pp. 157–63
38. Brown, T. M. 1985. *Nature* 317: 591–94
39. Brown, T. M. 1988. In AARHUS, pp. 453–65
40. Brown, T. M. 1991. In *Frontiers of Stellar Evolution*, ed. D. L. Lambert. San Francisco: Astron. Soc. Pac. In press
41. Brown, T. M. 1991. *Ap. J.* 371: 396–401
42. Brown, T. M., Christensen-Dalsgaard, J., Dziembowski, W. A., Goode, P. R., Gough, D. O., Morrow, C. A. 1989. *Ap. J.* 343: 526–46
43. Brown, T. M., Mihalas, B. W., Rhodes, E. J. Jr. 1986. In *Physics of the Sun. Vol. I: The Solar Interior*, ed. P. A. Sturrock, T. E. Holzer, D. M. Mihalas, R. K. Ulrich, pp. 171–247. Dordrecht: Reidel
44. Brown, T. M., Morrow, C. A. 1987. *Ap. J. Lett.* 314: L21–26
45. Cattaneo, F., Brummell, N. H., Toomre, J., Malagoli, A., Hurlburt, N. E. 1991. *Ap. J.* 370: 282–94
46. Cattaneo, F., Hurlburt, N. E., Toomre, J. 1990. *Ap. J. Lett.* 349: L63–66
47. Campbell, W. R., Roberts, B. 1989. *Ap. J.* 338: 538–56
48. Chandrasekhar, S. 1964. *Ap. J.* 139: 664–74
49. Christensen-Dalsgaard, J. 1982. *MNRAS* 199: 735–61
50. Christensen-Dalsgaard, J. 1984. In *Space Research Prospects in Stellar Activity and Variability*, ed. A. Mangeney, F. Praderie, pp. 11–45. Paris: Observatoire de Paris
51. Christensen-Dalsgaard, J. 1986. In CAMBRIDGE, pp. 23–53
52. Christensen-Dalsgaard, J. 1988. In AARHUS, pp. 295–98
53. Christensen-Dalsgaard, J. 1990. In VERSAILLES, pp. 305–26
54. Christensen-Dalsgaard, J. 1991. In ITP, pp. 11–36
55. Christensen-Dalsgaard, J. 1991. In *Solar Interior and Atmosphere*, ed. A. N. Cox, W. C. Livingston, M. Matthews. Tucson: Univ. Arizona Press. In press
56. Christensen-Dalsgaard, J., Berthomieu, G. 1991. In *Solar Interior and Atmosphere*, ed. A. N. Cox, W. C. Livingston, M. Matthews. Tucson: Univ. Arizona Press. In press
57. Christensen-Dalsgaard, J., Cooper, A. J., Gough, D. O. 1983. *MNRAS* 203: 165–79
58. Christensen-Dalsgaard, J., Däppen, W., Lebreton, Y. 1988. *Nature* 336: 634–38
59. Christensen-Dalsgaard, J., Dilke, F. W. W., Gough, D. O. 1974. *MNRAS* 169: 429–45
60. Christensen-Dalsgaard, J., Duvall, T. L. Jr., Gough, D. O., Harvey, J. W., Rhodes, E. J. Jr. 1985. *Nature* 315: 378–82
61. Christensen-Dalsgaard, J., Dziembowski, W. A., Gough, D. O. 1980. In *Nonradial and Nonlinear Stellar Pulsation*, ed. H. A. Hill, W. A. Dziembowski, pp. 313–41. Heidelberg: Springer
62. Christensen-Dalsgaard, J., Frandsen, S. 1983. *Sol. Phys.* 82: 165–204
63. Christensen-Dalsgaard, J., Frandsen, S. 1983. *Sol. Phys.* 82: 469–86
64. Christensen-Dalsgaard, J., Gough, D. O. 1980. *Nature* 288: 544–47
65. Christensen-Dalsgaard, J., Gough, D. O. 1981. *Astron. Astrophys.* 104: 173–76
66. Christensen-Dalsgaard, J., Gough, D. O. 1984. In SNOWMASS, pp. 79–93
67. Christensen-Dalsgaard, J., Gough, D. O., Libbrecht, K. G. 1989. *Ap. J. Lett.* 341: L103–6
68. Christensen-Dalsgaard, J., Gough, D. O., Thompson, M. J. 1989. *MNRAS* 238: 481–502
69. Christensen-Dalsgaard, J., Gough, D. O., Thompson, M. J. 1991. *Ap. J.* In press
70. Christensen-Dalsgaard, J., Gough, D. O., Toomre, J. 1985. *Science* 229: 923–31
71. Christensen-Dalsgaard, J., Pérez Hernández, F. 1988. In TENERIFE, pp. 499–503
72. Christensen-Dalsgaard, J., Pérez Hernández, F. 1991. In ITP, pp. 43–50

73. Christensen-Dalsgaard, J., Schou, J. 1988. In TENERIFE, pp. 149–53
74. Christensen-Dalsgaard, J., Schou, J., Thompson, M. J. 1990. *MNRAS* 242: 353–69
75. Claverie, A., Isaak, G. R., McLeod, C. P., van der Raay, H. B., Roca Cortés, T. 1979. *Nature* 282: 591–94
76. Claverie, A., Isaak, G. R., McLeod, C. P., van der Raay, H. B., Roca Cortés, T. 1981. *Nature* 293: 443–45
77. Cochran, W. D. 1988. *Ap. J.* 334: 349–56
78. Cowling, T. G. 1941. *MNRAS* 101: 367–75
79. Cox, A. N., Guzik, J. A., Kidman, R. B. 1989. *Ap. J.* 342: 1187–1206
80. Cox, A. N., Guzik, J. A., Raby, S. 1990. *Ap. J.* 353: 698–711
81. Cox, J. P. 1980. *Theory of Stellar Pulsation*. Princeton: Princeton Univ. Press
82. Dame, L. 1988. In TENERIFE, pp. 367–70
83. Däppen, W. 1990. In VERSAILLES, pp. 357–70
84. Däppen, W. 1990. In HAKONE, pp. 33–40
85. Däppen, W., Dziembowski, W. A., Sienkiewicz, R. 1988. In AARHUS, pp. 233–47
86. Däppen, W., Gough, D. O. 1984. In *Theoretical Problems in Stellar Stability and Oscillations*, ed. M. Gabriel, A. Noels, pp. 264–69. Liège: Institute d’Astrophysique
87. Däppen, W., Gough, D. O., Kosovichev, A. G., Thompson, M. J. 1991. In ITP, pp. 111–120
88. Däppen, W., Gough, D. O., Thompson, M. J. 1988. In TENERIFE, pp. 505–10
89. Däppen, W., Lebreton, Y., Rogers, F. J. 1990. *Sol. Phys.* 128: 35–47
90. Davis, R. Jr. 1988. In *Proc. Seventh Workshop on Grand Unification, ICOBAN ’86*, ed. J. Arafone, pp. 237–76. World Scientific
91. Davis, R. Jr., Lande, K., Lee, C. K., Cleveland, B. T., Ullman, J. 1990. In VERSAILLES, pp. 171–77
92. Demarque, P., Guenther, D. B. 1988. In AARHUS, pp. 91–94
93. Demarque, P., Guenther, D. B. 1990. In HAKONE, pp. 405–15
94. Deubner, F. L. 1975. *Astron. Astrophys.* 44: 371–75
95. Deubner, F. L., Gough, D. O. 1984. *Annu. Rev. Astron. Astrophys.* 22: 593–619
96. Duvall, T. L. Jr. 1982. *Nature* 300: 242–43
97. Duvall, T. L. Jr., Dziembowski, W. A., Goode, P. R., Gough, D. O., Harvey, J. W., Leibacher, J. W. 1984. *Nature* 310: 22–25
98. Duvall, T. L. Jr., Harvey, J. W. 1983. *Nature* 302: 24–27
99. Duvall, T. L. Jr., Harvey, J. W. 1984. *Nature* 310: 19–22
100. Duvall, T. L. Jr., Harvey, J. W., Libbrecht, K. G., Popp, B. D., Pomerantz, M. A. 1988. *Ap. J.* 324: 1158–71
101. Duvall, T. L. Jr., Harvey, J. W., Pomerantz, M. A. 1986. *Nature* 321: 500–1
102. Duvall, T. L. Jr., Harvey, J. W., Pomerantz, M. A. 1988. In AARHUS, pp. 37–40
103. Dziembowski, W. A. 1983. *Sol. Phys.* 82: 259–66
104. Dziembowski, W. A. 1984. *Adv. Space Res.* 4: 143–50
105. Dziembowski, W. A. 1990. In HAKONE, pp. 359–71
106. Dziembowski, W. A., Goode, P. R. 1989. *Ap. J.* 347: 540–50
107. Dziembowski, W. A., Goode, P. R. 1990. In VERSAILLES, pp. 341–48
108. Dziembowski, W. A., Goode, P. R. 1991. *Ap. J.* In press
109. Dziembowski, W. A., Goode, P. R., Libbrecht, K. G. 1989. *Ap. J.* 337: L53–57
110. Dziembowski, W. A., Gough, D. O. 1991. *MNRAS*. Submitted
111. Dziembowski, W. A., Pamyatnykh, A. A. 1978. In *Pleins Feux sur la Physique Solaire*, ed. S. Dumont, J. Rösch, pp. 135–40. Paris: CNRS
112. Dziembowski, W. A., Pamyatnykh, A. A., Sienkiewicz, R. 1990. *MNRAS* 244: 542–50
113. Dziembowski, W. A., Pamyatnykh, A. A., Sienkiewicz, R. 1991. *MNRAS* 249: 602–5
114. Eckart, C. 1960. *Hydrodynamics of Oceans and Atmospheres*. London: Pergamon
115. Ellis, A. N. 1986. In CAMBRIDGE, pp. 173–75
116. Ellis, A. N. 1988. In AARHUS, pp. 147–50
117. Elsworth, Y., Howe, R., Isaak, G. R., McLeod, C. P., New, R. 1990. *Nature* 347: 536–39
118. Elsworth, Y., Howe, R., Isaak, G. R., McLeod, C. P., New, R. 1990. *Nature* 345: 322–24
119. Elsworth, Y., Howe, R., Isaak, G. R., McLeod, C. P., New, R. 1991. *MNRAS*. Submitted
120. Elsworth, Y., Isaak, G. R., Jefferies, S. M., McLeod, C. P., New, R., Pallé, P. L., Régulo, C., Roca Cortés, T. 1988. In TENERIFE, pp. 27–29

121. Evans, D. J., Roberts, B. 1990. *Ap. J.* 356: 704–19
122. Filippone, B., Vogel, P. 1990. *Phys. Lett. B* 246: 546–50
123. Foing, B., Catala, C. 1990. In HAKONE, pp. 457–62
124. Fossat, E. 1988. In TENERIFE, pp. 161–62
125. Fossat, E., Gelly, B., Grec, C. 1986. In CAMBRIDGE, pp. 405–16
126. Fossat, E., Grec, C., Gelly, B., Decanini, Y. C. 1984. *Acad. Sci. Paris Ser. 2* 229: 17–20
- 127a. Frazier, E. N. 1968. *Z. Astrophys.* 68: 345–56
127. Fröhlich, C. 1990. In HAKONE, pp. 221–26
128. Fröhlich, C., Andersen, B. N., Berthomieu, G., Crommelynck, D., Delache, P., Domingo, V., Jimenes, A., Jones, A. R., Roca Cortés, T., Wehrli, C. 1988. In TENERIFE, pp. 371–74
129. Fröhlich, C., Toutain, T. 1990. In HAKONE, pp. 215–20
130. Fröhlich, C., Toutain, T., Bonnet, R. M., Bruns, A. V., Delaboudiniere, J. P., Domingo, V., Kotov, V. A., Kollath, Z., Rashkovsky, D. N., Vial, J. C., Wehrli, C. 1991. *Nature*
131. Gabriel, M. 1986. In CAMBRIDGE, pp. 177–86
132. Gabriel, M. 1990. In HAKONE, pp. 23–31
133. Gabriel, M. 1991. In ITP, pp. 51–55
134. Garcia, C., Pallé, P. L., Roca Cortés, T. 1988. In TENERIFE, pp. 353–57
135. Gavrin, V. N. 1991. *Ann. NY Acad. Sci.* In press
136. Gelly, B., Fossat, E., Grec, G. 1988. In TENERIFE, pp. 275–77
137. Gelly, B., Fossat, E., Grec, G., Pomerantz, M. 1988. In AARHUS, pp. 21–23
138. Gilliland, R. L., Brown, T. M. 1988. *Publ. Astron. Soc. Pac.* 100: 754–65
139. Goldreich, P., Keeley, D. A. 1977. *Ap. J.* 211: 934–42
140. Goldreich, P., Keeley, D. A. 1977. *Ap. J.* 212: 243–51
141. Goldreich, P., Kumar, P. 1988. *Ap. J.* 326: 462–78
142. Goldreich, P., Kumar, P. 1990. *Ap. J.* 363: 694–704
143. Goldreich, P., Murray, N., Willette, G., Kumar, P. 1991. *Ap. J.* In press
144. Goode, P. R., Dziembowski, W. A. 1991. *Nature* 349: 223–25
145. Goode, P. R., Dziembowski, W. A., Rhodes, E. J. Jr., Korzennik, S. G. 1990. In HAKONE, pp. 349–52
146. Goode, P. R., Kuhn, J. R. 1990. *Ap. J.* 356: 310–14
147. Gough, D. O. 1976. In *The Energy Balance and Hydrodynamics of the Solar Chromosphere and Corona*, ed. R. M. Bonnet, P. Delache, pp. 3–36. Clermont-Ferrand: G. de Bussac
148. Gough, D. O. 1978. In *Pleins Feux sur la Physique Solaire*, ed. S. Dumont, J. Rösch, pp. 81–103. Paris: CNRS
149. Gough, D. O. 1980. In *Nonradial and Nonlinear Stellar Oscillations*, ed. H. A. Hill, W. A. Dziembowski, pp. 273–99. Heidelberg: Springer
150. Gough, D. O. 1983. *Phys. Bull.* 34: 502–6
151. Gough, D. O. 1984. *Adv. Space Res.* 4: 85–102
152. Gough, D. O. 1984. *Philos. Trans. R. Soc. London Ser. A* 313: 27–38
153. Gough, D. O. 1984. *Mem. Soc. Astron. Ital.* 55: 13–35
154. Gough, D. O. 1985. *Sol. Phys.* 100: 65–99
155. Gough, D. O. 1985. In *Future Missions in Solar, Heliospheric and Space Plasma Physics*, ed. E. J. Rolfe, pp. 183–97. ESA SP-235. Noordwijk: ESA ESTEC
156. Gough, D. O. 1986. In CAMBRIDGE, pp. 125–40
157. Gough, D. O. 1986. In *Hydrodynamic and Magnetohydrodynamic Problems in the Sun and Stars*, ed. Y. Osaki, pp. 117–43. Tokyo: Univ. Tokyo Press
158. Gough, D. O. 1987. *Nature* 326: 257–59
159. Gough, D. O. 1988. *Nature* 336: 720
160. Gough, D. O. 1991. In *Astrophysical Fluid Dynamics, Les Houches XLVII*, 1987, ed. J.-P. Zahn, J. Zinn-Justin. Amsterdam: Elsevier. In press
161. Gough, D. O., Kosovichev, A. G. 1988. In TENERIFE, pp. 195–201
162. Gough, D. O., Kosovichev, A. G. 1990. In VERSAILLES, pp. 327–40
163. Gough, D. O., Merryfield, W. J., Toomre, J. 1991. In ITP, pp. 265–70
164. Gough, D. O., Novotny, E. 1990. *Solar Phys.* 128: 143–60
165. Gough, D. O., Thompson, M. J. 1988. In AARHUS, pp. 175–80
166. Gough, D. O., Thompson, M. J. 1990. *MNRAS* 242: 25–55
167. Gough, D. O., Thompson, M. J. 1991. In *Solar Interior and Atmosphere*, ed. A. N. Cox, W. C. Livingston, M. Matthews. Tucson: Univ. Arizona Press. In press
168. Gough, D. O., Toomre, J. 1983. *Sol. Phys.* 82: 401–10
169. Gough, D. O., Toomre, J. 1988. *GONG Newsletter* 9: 20–60
170. Gough, D. O., Weiss, N. O. 1976. *MNRAS* 176: 589–607
171. Grec, G., Fossat, E., Pomerantz, M. 1980. *Nature* 288: 541–44

172. Haber, D. A., Hill, F. 1991. In ITP, pp. 253–58
173. Haber, D. A., Hill, F., Toomre, J. 1991. In ITP, pp. 87–92
174. Haber, D. A., Hill, F., Toomre, J. 1991. In ITP, pp. 259–64
175. Haber, D. A., Toomre, J., Hill, F. 1988. In AARHUS, pp. 59–62
176. Harari, H. 1990. In VERSAILLES, pp. 213–30
177. Harvey, J. W. 1988. In AARHUS, pp. 497–511
178. Harvey, J. W. 1990. In HAKONE, pp. 115–28
179. Harvey, J. W., Duvall, T. L. Jr. 1984. In SNOWMASS, pp. 165–72
180. Harvey, J. W., GONG Instrument Development Team 1988. In TENERIFE, pp. 203–8
181. Harvey, J. W., Kennedy, J. R., Leibacher, J. W. 1987. *Sky & Telescope* 74: 470–76
182. Henning, H. M., Scherrer, P. H. 1988. In AARHUS, pp. 29–32
183. Hill, F. 1988. *Ap. J.* 333: 996–1013
184. Hill, F. 1989. *Ap. J. Lett.* 343: L69–71
185. Hill, F. 1990. In VERSAILLES, pp. 265–78
186. Hill, F. 1990. *Sol. Phys.* 128: 321–31
187. Hill, F. 1990. In HAKONE, pp. 173–79
188. Hill, F., GONG Site Survey Team 1988. In TENERIFE, pp. 209–15
189. Hill, F., Gough, D. O., Merryfield, W. J., Toomre, J. 1991. *Ap. J.* 369: 237–46
190. Hill, F., Gough, D. O., Toomre, J., Haber, H. A. 1988. In AARHUS, pp. 45–48
191. Hill, F., Haber, D. A., Toomre, J., November, L. J. 1988. In CAMBRIDGE, pp. 85–92
192. Hill, F., Rust, D. M., Appourchaux, T. 1988. In AARHUS, pp. 49–52
193. Hill, F., Toomre, J., Gough, D. O. 1984. In SNOWMASS, pp. 95–111
194. Hill, H. A., Gao, Q., Rosenwald, R. D. 1988. In TENERIFE, pp. 403–6
195. Hill, H. A., Stebbins, R. T., Brown, T. M. 1976. In *Atomic Masses and Fundamental Constants*, ed. J. H. Sanders, A. H. Wapstra, pp. 622–28. New York: Plenum
196. Hirata, K. S., Kamiokande-II Collaboration 1990. In VERSAILLES, pp. 179–86
197. Hoeksema, J. T., Scherrer, P. H., Title, A. M., Tarbell, T. D. 1988. In TENERIFE, pp. 407–12
198. Hollweg, J. V. 1988. *Ap. J.* 335: 1005–14
199. Hoyle, F. 1975. *Ap. J. Lett.* 197: L127–37
200. Hummer, D. G., Mihalas, D. 1988. *Ap. J.* 331: 794–814
201. Iben, I. Jr. 1974. *Annu. Rev. Astron. Astrophys.* 12: 215–56
202. Iglesias, C. A., Rogers, F. J. 1990. In VERSAILLES, pp. 81–90
203. Iglesias, C. A., Rogers, F. J., Wilson, B. G. 1987. *Ap. J. Lett.* 322: L45–48
204. Innes, J. L., Isaak, G. R., Brazier, R. I., Belmonte, J. A., Pallé, P. L., Roca Cortés, T. 1988. In TENERIFE, pp. 569–73
205. Irwin, A. W., Campbell, B., Morbey, C. L., Walker, G. A. H., Yang, S. 1989. *Publ. Astron. Soc. Pac.* 101: 147–59
206. Isaak, G. R., McLeod, C. P., van der Raay, H. B., Pallé, P. L., Roca Cortés, T. 1988. In AARHUS, pp. 53–57
207. Jefferies, S. M., Duvall, T. L. Jr., Harvey, J. W., Pomerantz, M. A. 1990. In HAKONE, pp. 135–44
208. Jefferies, S. M., Pomerantz, M. A., Duvall, T. L. Jr., Harvey, J. W., Jaksha, D. B. 1988. In TENERIFE, pp. 279–84
209. Jones, P. W., Merryfield, W. J., Toomre, J. 1991. In ITP, pp. 213–20
210. Jones, P. W., Merryfield, W. J., Toomre, J. 1991. *Ap. J.* Submitted
211. Kawaler, S. D. 1991. In ITP, pp. 309–24
212. Keller, J. B., Rubinow, S. I. 1960. *Ann. Phys.* 9: 24–75
213. Korzennik, S. G., Cacciani, A., Rhodes, E. J. Jr., Ulrich, R. K. 1990. In HAKONE, pp. 341–47
214. Korzennik, S. G., Ulrich, R. K. 1989. *Ap. J.* 339: 1144–55
215. Kosovichev, A. G. 1988. In TENERIFE, pp. 533–37
216. Kosovichev, A. G., Parchevskii, K. V. 1988. *Pis'ma Astron. Zh.* 14: 473–80
217. Krastev, P. I., Mikheyev, S. P., Smirnow, A. Yu. 1991. In *Low Energy Weak Interactions School (Dubna, USSR 3–14 Sept. 1990)*. In press
218. Krauss, L. M. 1990. *Nature* 348: 403–7
219. Kuhn, J. R. 1988. *Ap. J. Lett.* 331: L131–34
220. Kuhn, J. R. 1988. In TENERIFE, pp. 87–90
221. Kuhn, J. R., Libbrecht, K. G., Dicke, R. H. 1988. *Science* 242: 908–11
222. Kumar, P., Franklin, J., Goldreich, P. 1988. *Ap. J.* 328: 879–87
223. Kumar, P., Goldreich, P. 1989. *Ap. J.* 342: 558–75
224. Kurtz, D. W. 1990. In HAKONE, pp. 373–83
225. Larson, R. B. 1969. *MNRAS* 145: 271–95
226. Lavelle, E. M., Ritzwoller, M. H. 1991. *Ap. J.* 369: 557–66

227. Ledoux, P., Walraven, Th. 1957. *Handbuch der Physik.* 51: 353–604
228. Leibacher, J. W., Noyes, R. W., Toomre, J., Ulrich, R. K. 1985. *Scientific Amer.* 253(3): 48–57
229. Leibacher, J. W., Stein, R. F. 1971. *Astrophys. Lett.* 7: 191–92
230. Leighton, R. B. 1960. *Proc. IAU Symp. No. 12*, pp. 321–25
231. Leighton, R. B., Noyes, R. W., Simon, G. W. 1962. *Ap. J.* 135: 474–99
232. Libbrecht, K. G. 1988. *Space Sci. Rev.* 47: 275–301
233. Libbrecht, K. G. 1988. *Ap. J.* 334: 510–16
234. Libbrecht, K. G. 1988. In TENERIFE, pp. 3–10
235. Libbrecht, K. G. 1989. *Ap. J.* 336: 1092–97
236. Libbrecht, K. G., Kaufman, J. M. 1988. *Ap. J.* 324: 1172–83
237. Libbrecht, K. G., Kaufman, J. M. 1991. *Ap. J. Suppl.* In press
238. Libbrecht, K. G., Popp, B. D., Kaufman, J. M., Penn, M. J. 1986. *Nature* 323: 235–38
239. Libbrecht, K. G., Woodard, M. F. 1990. *Nature* 345: 779–82
240. Libbrecht, K. G., Woodard, M. F. 1990. In HAKONE, pp. 145–56
241. Libbrecht, K. G., Woodard, M. F., Kaufman, J. M. 1990. *Ap. J. Suppl.* 74: 1129–49
242. Libbrecht, K. G., Zirin, H. 1986. *Ap. J.* 308: 413–23
243. Lighthill, M. J. 1952. *Proc. R. Soc. London Ser. A* 211: 564–87
244. Lighthill, M. J. 1954. *Proc. R. Soc. London Ser. A* 222: 1–32
245. Loeb, A., Bahcall, J. N., Milgrom, M. 1989. *Ap. J.* 341: 1108–13
246. Lou, Y.-Q. 1988. In TENERIFE, pp. 305–10
247. Malagoli, A., Cattaneo, F., Brummell, N. H. 1990. *Ap. J. Lett.* 361: L33–36
248. Merryfield, W. J., Toomre, J. 1991. *Ap. J.* Submitted
249. Merryfield, W. J., Toomre, J., Gough, D. O. 1988. In TENERIFE, pp. 21–26
250. Merryfield, W. J., Toomre, J., Gough, D. O. 1990. *Ap. J.* 353: 678–97
251. Merryfield, W. J., Toomre, J., Gough, D. O. 1991. *Ap. J.* 367: 658–65
252. Mihalas, D., Däppen, W., Hummer, D. G. 1988. *Ap. J.* 331: 815–25
253. Mikheyev, S. P., Smirnov, A. Yu. 1985. *Sov. J. Nucl. Phys.* 42: 913–19
254. Morel, P., Provost, J., Berthomieu, G. 1990. *Sol. Phys.* 128: 7–20
255. Noyes, R. W., Baliunas, S. L., Belserene, E., Duncan, D. K., Horne, J., Widrow, L. 1984. *Ap. J. Lett.* 285: L23–26
256. Osaki, Y. 1975. *Publ. Astron. Soc. Jpn.* 27: 237–58
257. Osaki, Y. 1990. In HAKONE, pp. 75–86
258. Pallé, P. L., Pérez Hernández, F., Roca Cortés, T., Isaak, G. R. 1989. *Astron. Astrophys.* 216: 253–58
259. Pallé, P. L., Régulo, C., Roca Cortés, T. 1990. In HAKONE, pp. 129–34
260. Parker, E. N. 1987. *Ap. J.* 321: 984–1008
261. Perdang, J. 1986. In CAMBRIDGE, pp. 141–71
262. Perdang, J. 1991. In ITP, pp. 135–40
263. Perrin, M. N., Cyrel de Strobel, G., Dennefeld, M. 1988. *Astron. Astrophys.* 191: 237–47
264. Provost, J. 1984. In *Observational Tests of Stellar Evolution Theory*, ed. A. Maeder, A. Renzini, pp. 47–64. Dordrecht: Reidel
265. Provost, J., Berthomieu, G. 1986. *Astron. Astrophys.* 165: 218–26
266. van der Raay, H. B. 1988. In TENERIFE, pp. 339–51
267. Rhodes, E. J. Jr., Cacciani, A., Korzennik, S. 1988. In TENERIFE, pp. 81–86
268. Rhodes, E. J. Jr., Cacciani, A., Korzennik, S. 1990. In HAKONE, pp. 163–72
269. Rhodes, E. J. Jr., Cacciani, A., Korzennik, S., Ulrich, R. K. 1991. In ITP, pp. 285–92
270. Rhodes, E. J. Jr., Cacciani, A., Tomczyk, S., Ulrich, R. K. 1986. In CAMBRIDGE, pp. 309–32
271. Rhodes, E. J. Jr., Woodard, M. F., Cacciani, A., Tomczyk, S., Korzennik, S. G., Ulrich, R. K. 1988. *Ap. J.* 326: 479–85
272. Roberts, B., Campbell, W. R. 1986. *Nature* 323: 603–5
273. Rogers, F. J. 1986. *Ap. J.* 310: 723–28
274. Rosen, S. P., Gelb, J. M. 1986. *Phys. Rev. D* 34: 969–79
275. Rosenthal, C. S. 1990. *Sol. Phys.* 130: 313–35
276. Rosenthal, C. S., Gough, D. O. 1988. In TENERIFE, pp. 457–61
277. Roxburgh, I. W. 1985. *Sol. Phys.* 100: 21–51
278. Roxburgh, I. W. 1987. In *The Internal Solar Angular Velocity*, ed. B. R. Durney, S. Sofia, pp. 1–5. Dordrecht: Reidel
279. Rust, D. M., Appourchaux, T., Hill, F. 1988. In AARHUS, pp. 475–79
280. Saio, H. 1980. *Ap. J.* 240: 685–92
281. Scherrer, P. H., Hoeksema, J. T., Bogart, R. S., SOI Co-I Team 1988. In TENERIFE, pp. 375–79

282. Schmider, F.-X., Fossat, E., Gelly, B., Grec, G. 1990. In HAKONE, pp. 241–51
283. Schmitt, J. H. M., Rosner, R., Bohn, H. V. 1984. *Ap. J.* 282: 316–29
284. Schou, J. 1991. In ITP, pp. 81–86
285. Schou, J. 1991. In ITP, pp. 93–100
286. Scuflaire, R. 1974. *Astron. Astrophys.* 36: 107–11
287. Sekii, T. 1990. In HAKONE, pp. 337–40
288. Sekii, T. 1991. *Publ. Astron. Soc. Jpn.* In press
289. Sekii, T., Shibahashi, H. 1989. *Publ. Astron. Soc. Jpn.* 41: 311–31
290. Severney, A. B., Kotov, V. A., Tsap, T. T. 1976. *Nature* 259: 87–89
291. Severney, A. B., Kotov, V. A., Tsap, T. T. 1988. In AARHUS, pp. 33–36
292. Shapiro, I. I., Counselman, C. C. III, King, R. W. 1976. *Phys. Rev. Lett.* 36: 555–58
293. Shibahashi, H. 1979. *Publ. Astron. Soc. Jpn.* 31: 87–104
294. Shibahashi, H. 1987. In AARHUS, pp. 133–36
295. Shibahashi, H. 1990. In HAKONE, pp. 3–19
296. Shibahashi, H., Noels, A., Gabriel, M. 1983. *Astron. Astrophys.* 123: 283–88
297. Shibahashi, H., Osaki, Y., Unno, W. 1975. *Publ. Astron. Soc. Jpn.* 27: 401–10
298. Shibahashi, H., Sekii, T. 1988. In TENERIFE, pp. 471–74
299. Smirnov, A. Yu. 1990. In VER-SAILLES, pp. 231–50
300. Smith, G., Evardsson, B., Frisk, U. 1986. *Astron. Astrophys.* 165: 126–34
301. Smith, P. H., MacMillan, R. S., Merline, W. J. 1985. *Ap. J. Lett.* 317: L79–84
302. Spiegel, E. A., Weiss, N. O. 1980. *Nature* 287: 616–17
303. Spiro, M., Vignaud, D. 1990. In VER-SAILLES, pp. 157–69
304. Spite, F., Spite, M., François, P. 1989. *Astron. Astrophys.* 210: 25–34
305. Spruit, H. C. 1991. In ITP, pp. 121–34
306. Stein, R. F. 1967. *Sol. Phys.* 2: 385–432
307. Stein, R. F., Nordlund, Å. 1990. In HAKONE, pp. 93–102
308. Stein, R. F., Nordlund, Å. 1991. In ITP, pp. 195–212
309. Tassoul, J.-L. 1978. *Theory of Rotating Stars*. Princeton: Princeton Univ. Press
310. Tassoul, M. 1980. *Ap. J. Suppl.* 43: 469–90
311. Tassoul, M. 1990. *Ap. J.* 358: 313–27
312. Thompson, M. J. 1989. *Sol. Phys.* 125: 1–12
313. Thompson, M. J. 1991. In ITP, pp. 61–80
314. Toomre, J. 1984. In SNOWMASS, pp. 7–39
315. Toomre, J. 1986. In CAMBRIDGE, pp. 1–22
316. Toomre, J., Brummell, N. H., Cattaneo, F. 1990. *Comp. Phys. Comm.* 59: 105–17
317. Ulrich, R. K. 1970. *Ap. J.* 162: 993–1002
318. Ulrich, R. K. 1986. In CAMBRIDGE, pp. 187–98
319. Ulrich, R. K. 1986. *Ap. J. Lett.* 306: L37–40
320. Ulrich, R. K. 1988. In AARHUS, pp. 299–302
321. Unno, W. 1964. *Trans. IAU* 12B: 555–58
322. Unno, W., Osaki, Y., Ando, H., Shibahashi, H. 1989. *Nonradial Oscillations of Stars*. Tokyo: Univ. Tokyo Press. 2nd ed.
- 322a. van Ballegooijen, A. 1982. *Astron. Astrophys.* 113: 99–112
323. Vauclair, S., Charbonnel, C. 1991. In ITP, pp. 37–41
324. Vorontsov, S. V. 1988. In TENERIFE, pp. 475–80
325. Vorontsov, S. V. 1990. In HAKONE, pp. 67–74
326. Vorontsov, S. V., Baturin, V. A., Pamyatnykh, A. A. 1991. *Nature* 349: 49–51
327. Vorontsov, S. V., Zharkov, V. N. 1989. *Sov. Sci. Rev. E. Astrophys. Space Phys.* 7: 1–103
328. Wambeganass, J. 1988. *Astron. Astrophys.* 205: 125–28
329. Wheeler, J. C., Cameron, A. G. W. 1975. *Ap. J.* 196: 601–5
330. Will, C. M. 1990. *Science* 250: 770–76
331. Willson, R. C., Hudson, H. S. 1988. *Nature* 332: 810–12
332. Wolfenstein, L. 1978. *Phys. Rev. D* 17: 2369–74
333. Woodard, M. F. 1989. *Ap. J.* 347: 1176–82
334. Woodard, M. F., Hudson, H. S. 1983. *Nature* 305: 589–93
335. Woodard, M. F., Hudson, H. S. 1984. *Mem. Soc. Astron. Ital.* 55: 67–68
336. Woodard, M. F., Noyes, R. W. 1985. *Nature* 318: 449–50
337. Zahn, J.-P. 1970. *Astron. Astrophys.* 4: 452–61
338. Zweibel, E. G., Bogdan, T. J. 1986. *Ap. J.* 308: 401–12
339. Zweibel, E. G., Däppen, W. 1989. *Ap. J.* 343: 994–1003

References added in proof

- 42a. Brown, T. M., Gilliland, R. L., Noyes, R. W., Ramsey, L. W. 1991. *Ap. J.* 368: 599–609
- 52a. Christensen-Dalsgaard, J. 1988. In TENERIFE, pp. 431–50
- 99a. Duvall, T. L. Jr., Harvey, J. W., Jeffries, S. M., Pomerantz, M. A. 1991. *Ap. J.* 373: 308–16
- 130a. Fukugita, M., Yanagida, T. 1991. *Mod. Phys. Lett. A* 6: 645–57
- 137a. Gelly, B., Fossat, E., Grec, G., Schmider, F.-X. 1988. *Astron. Astrophys.* 200: 207–12
- 138a. Gilliland, R. L., Faulkner, J., Press, W. H., Spergal, D. N. 1986. *Ap. J.* 306: 703–9
- 159a. Gough, D. O. 1990. In HAKONE, pp. 283–318
- 202a. Iglesias, C. A., Rogers, F. J. 1991. *Ap. J. Lett.* 371: L73–L75
- 215a. Kosovichev, A. G., Fedorova, A. V. 1991. *Astron. Zh.* In press
- 216a. Kosovichev, A. G., Severny, A. B. 1985. *Izv. Krymsk. Astrofiz. Obs.* 72: 188–98